Title

I. NEUTRON-DEFICIENT ISOTOPES IN THE NOBLE MEDAL REGION. II. CONVERSION ELECTRON SPECTRA OF SOME HEAVY ELEMENTS

Author

Smith, Warren G.

Publication Date

1955-06-01

UNIVERSITY OF CALIFORNIA

Radiation Laboratory

BERKELEY, CALIFORNIA

DISCLAIMER

UCRL-2974

UNIVERSITY OF CALIFORNIA
Radiation Laboratory
Berkeley, California

Contract No. W-7405-eng-48

I NEUTRON-DEFICIENT ISOTOPES IN THE NOBLE METAL REGION
II CONVERSION ELECTRON SPECTRA OF SOME HEAVY ELEMENTS

Warren G. Smith

(Thesis)

June 1955

Printed for the U. S. Atomic Energy Commission

TABLE OF CONTENTS

I Neutron-Deficient Isotopes in the Noble Metal Region
II Conversion Electron Spectra of Some Heavy Elements

Warren G. Smith
Radiation Laboratory and Department of Chemistry
University of California, Berkeley, California

June 1955

ABSTRACT

Part I

A radiochemical study of some neutron-deficient nuclides in the noble metal region has been undertaken, and several new chains identified. The method used to establish genetic relationships was that of timed chemical separations, where the parent activities are initially produced by cyclotron or linear accelerator bombardments. The following chains have been identified:

A = 191: $Hg^{191} \xrightarrow{55\ min} Au^{191} \xrightarrow{3.0\ hr} Pt^{191} \xrightarrow{3.0\ day} Ir^{191}$

A = 189: $Hg^{189} \xrightarrow{\sim 20\ min} Au^{189} \xrightarrow{42\ min} Pt^{189} \xrightarrow{10.5\ hr} Ir^{189} \xrightarrow{11\ day(?)} Os^{189}$

A = 188: $Pt^{188} \xrightarrow{10.0\ day} Ir^{188} \xrightarrow{41\ hr} Os^{188}$

A = 187: $Au^{187} \xrightarrow{\sim 15\ min} Pt^{187} \xrightarrow{2.5\ hr} Ir^{187} \xrightarrow{14\ hr} Os^{187}$

Part II

Two 180° permanent magnet spectrographs with fields of approximately 50 and approximately 100 gauss were constructed and calibrated. These spectrographs have maximum electron radii of curvature of approximately 20 cm; the 50 gauss instrument will record electrons with energies up to approximately 85 kev, and the 100 gauss instrument will record up to approximately 275 kev. The 50 gauss spectrograph has a resolution of approximately 0.15 percent; the 100 gauss spectrograph has a resolution of approximately 0.3 percent. The spectrograph and auxiliary equipment are described.

The precise energies and the approximate intensities of the Auger electrons emitted in the decay of I^{131} were determined. The conversion

electrons emitted in transitions from the first excited state to the ground state of Pu^{238} and Pu^{240}, which are the decay products of Cm^{242} and Cm^{244}, respectively, were studied. The low-energy conversion electrons emitted in the alpha decay of Am^{241} were also investigated and some transition multipolarities are discussed.

I Neutron-Deficient Isotopes in the Noble Metal Region
II Conversion Electron Spectra of Some Heavy Elements

Warren G. Smith
Radiation Laboratory and Department of Chemistry
University of California, Berkeley, California

June 1955

Part I

I. INTRODUCTION

In this laboratory several isotopes of platinum and gold with mass numbers less than 191 had been observed in the course of other work, but a systematic radiochemical study of this region had not been pursued. In this paper the synthesis and identification of the following chains is reported:

$$Hg^{191} \rightarrow Au^{191} \rightarrow Pt^{191} \rightarrow Ir^{191}$$
$$Hg^{189} \rightarrow Au^{189} \rightarrow Pt^{189} \rightarrow Ir^{189} \rightarrow Os^{189}$$
$$Pt^{188} \rightarrow Ir^{188} \rightarrow Os^{188}$$
$$Au^{187} \rightarrow Pt^{187} \rightarrow Ir^{187} \rightarrow Os^{187} .$$

Recent energy level studies[1, 2, 3] of odd-mass nuclei in the region A = 191 through A = 197 have shown that interesting regularities exist in the movement of proton and neutron energy levels as pairs of nucleons of the other kind are added. The identification of these new isotopes of platinum and gold with $A \leq 191$ should permit the extension of nuclear spectroscopic measurements to this region.

II. EXPERIMENTAL PROCEDURES

A. Target Arrangements

The target materials used in this series of experiments consisted of metallic iridium, platinum, gold, and tantalum. The iridium targets used were in both the powder and foil forms. In both cases spectrographic analysis showed that the platinum content, which would be the only serious contaminant, was between 0.01 and 0.1 percent. Platinum black was used for the platinum targets, because this material is readily soluble in aqua regia. The platinum black was prepared by heating zinc to the molten state in a porcelain crucible and adding platinum foil which dissolved. The molten flux, along with the crucible, was plunged into approximately 6 M HCl and the zinc dissolved, leaving the finely powdered platinum. The platinum black was washed with concentrated HCl, water, and dried.

In the iridium and platinum powder bombardments, approximately 300 mg of target material was used. The powder was placed in an envelope made of 1-mil aluminum foil and then the envelope was placed in a holder suited to the accelerator being utilized. Two-mil iridium and 5-mil gold foils were used in these bombardments. One-quarter-mil tantalum foil was used for the carbon ion bombardments.

The stacked foil technique, which consists of alternate target and absorber foils, was used in the excitation functions.

It was not intended to determine any absolute cross sections, therefore no monitor foils were used except in the case of the excitation functions where a rough check was made of the beam current by using a polyethylene foil and the $C^{12}(p, pn)C^{11}$ reaction as a monitor.

B. Accelerators Used

1. 184-inch cyclotron. --Protons of 50- to 140-Mev energy obtained by using the internal probe were used. The powder targets were placed in aluminum envelopes for bombardment and the foils were bombarded directly.

2. 32-Mev linear accelerator. --Twenty-five- to 32-Mev protons were used. This machine was also used to perform some excitation function experiments on iridium foils. The target envelopes or foils were held in place on an aluminum plate with scotch tape.

3. 60-inch cyclotron. --Twelve-Mev protons were used to bombard iridium powder. Carbon ions were also used for a few bombardments.

C. Counting Techniques

Counting of the decay of the samples was done on an end-window, chlorine-quenched argon-filled Amperex-100c Geiger

counting tube, used in conjunction with a 256-scaling circuit. The samples were placed in a lucite sample holder with 5 shelves, and usually counted on the second from the top shelf, which had a shelf to window distance of 2.04 cm. The shelving arrangement and the Geiger tube were housed in a thick-walled lead container lined with aluminum to reduce background radiation and absorb secondary electrons.

Usually a sample which was a small fraction of the magnitude of the Geiger counter sample was prepared for gamma analysis with a sodium iodide (thallium activated) scintillation spectrometer coupled to a 50-channel differential analyzer. These gamma data were used to follow the decay of certain gamma peaks and/or x-rays and in addition were helpful in the identification of the various nuclides encountered, both old and new.

D. Chemical Procedures

The chemical procedures used were either techniques that are commonly in use or modifications of these techniques. The total target activity was as high as 100 roentgens at a distance of 2 inches when the chemical steps were begun, therefore the question of minimum exposure for the chemist had to be considered. All chemical operations (at least until the activity decreased to a safe level) were done with 3-foot long tongs passed through slots in a 2-inch thick lead brick wall, the whole system being built into a standard

ventilating hood. Strategically placed mirrors were used to observe some of the operations which were conducted behind the lead wall.

Platinum separation after proton bombardment of iridium. --A melt of an approximately 50-50 mixture of KOH and KNO_3, with a few mg of platinum and gold carrier added was heated strongly in a porcelain crucible with a Fisher burner. The target iridium metal, powder or foil, was added to the flux and heated for approximately 10 to 15 minutes. The flux was allowed to cool somewhat and while still moderately hot it was placed in a mortar, the crucible was broken and the semi-solid flux broken up with a pestle. It was then leached with concentrated HCl. The gold was removed and discarded by extracting three or more times with ethyl acetate. $SnCl_2$ was added to the aqueous phase until the dark red coloration of H_2PtCl_4 indicated that the reduction of platinum from the (+IV) to the (+II) state was complete. The red coloration was extracted three times into amyl acetate and washed 3 times with equal volumes of 3 M HCl. When time permitted and additional purification was desired the platinum organic phase was evaporated over 3 M HCl on a hot plate, iridium and gold carriers were added, and the extractions were repeated. The purified platinum was then either deposited directly on an aluminum counting plate or it was evaporated over aqua regia and $CsNO_3$ was added to precipitate cesium chloroplatinate. The latter was washed with 3 M HCl and deposited on a platinum plate for counting.

Gold separation after proton bombardment of platinum. --The platinum black was dissolved in a minimum amount of aqua regia with added tantalum, tungsten, rhenium, osmium, iridium, and gold carriers. The solution was evaporated to a small volume which distilled off OsO_4 and precipitated the oxides of tantalum, tungsten, and rhenium. After centrifuging, the oxide precipitate was discarded. After dilution to 5 ml the gold was extracted 3 times with 3 M HCl. The gold organic phase was used directly, evaporated over 3 M HCl and recycled, or after being evaporated over 1 M HCl, gold metal was precipitated from a hot solution by the addition of SO_2. The gold metal was sometimes dissolved in aqua regia and recycled for further purification.

Mercury separation after proton bombardment of gold. --The gold foil was dissolved in 5 ml of aqua regia with tantalum, tungsten, rhenium, osmium, iridium, platinum, and mercury carriers added. The solution was evaporated to 1 to 2 ml which distilled off OsO_4. After centrifuging, the precipitate of the oxides of tantalum, tungsten, and rhenium was discarded. The solution was diluted to 5 ml with 3 M HCl and the gold was extracted as many times as necessary into ethyl acetate. $SnCl_2$ was added to precipitate Hg_2Cl_2 and the latter was washed with 3 M HCl.

Gold separation after carbon ion bombardment of tantalum. --The tantalum foil was dissolved in 3 ml of HF plus a minimum amount

of concentrated HNO_3 which contained gold, platinum, tungsten, and iridium carriers. Three ml of concentrated HCl were added to make the Cl^- concentration approximately 6 M. Gold was extracted three times into amyl acetate, washed three times with 3 M HCl, and evaporated over 3 M HCl. The oxides of tungsten and tantalum precipitated and were centrifuged. Platinum and iridium carriers were added and the gold was extracted into amyl acetate and washed with 3 M HCl. Further gold purification was done in some cases.

Iridium milking from platinum. --No successful method was found for making timed iridium from platinum milkings, however it was possible to achieve fairly good separations by making multiple platinum extractions with an organic solvent. In order to effect this separation the purified platinum was evaporated over 3 M HCl with iridium carrier added and then allowed to decay for a desired length of time. The platinum was reduced to the (+II) state and extracted three times into ethyl acetate; more carrier was added and the process was repeated at least two more times. The iridium was left behind and was plated for counting. If it was desired to observe the decay and/or growth of the platinum fraction the organic phase was washed with 3 M HCl, recycled through an aqueous phase and prepared for counting as previously described.

Platinum milking from gold. --The purified gold was extracted into approximately 2 ml of ethyl acetate, one ml 3 M HCl with a

small amount of HNO_3 and platinum carrier was then added and thoroughly mixed with the organic phase. The two phases were separated by centrifuging. When the milking interval was long enough the platinum extraction was performed three times. The platinum aqueous phase was washed three times with ethyl acetate and an aliquot was plated directly for counting.

Gold milking from mercury. --The purified mercury fraction was dissolved in aqua regia and diluted to 3 ml with 3 M HCl. One ml of amyl acetate with gold carrier present was added to the mercury phase and thoroughly mixed. The mixture was centrifuged and the gold organic phase was removed and washed three times with 6 M HCl to remove any mercury present. An aliquot was plated directly for counting.

E. Isotope Identification Methods

In this work, targets of element Z were bombarded in general with protons from the 184-inch cyclotron to produce isotopes of element (Z + 1) by the (p, xn) reaction. The proton energy was varied between 50 and 140 Mev to bring in various values of x. Some excitation function experiments and proton bombardments were also performed with the 32-Mev proton beam of the Berkeley linear accelerator, and a few proton and heavy ion bombardments were made in the 60-inch cyclotron.

The Geiger counter decay curves of the primary (Z + 1) chemical fractions were in general so complex that their resolution was difficult at best and often unsuccessful. Consequently, half-lives and genetic chain relationships were often determined by means of the chemical "milking" technique introduced by Neumann and Perlman[4] and Karraker and Templeton.[5] In this method, chemical separations of daughter activities from the purified (Z + 1) fractions are made at a sequence of equal time intervals, the interval corresponding approximately to the expected half-life of the parent.

The number of atoms of a daughter substance present at a time t after purification of its parent is given by the formula

$$N_2 = \frac{\lambda_1}{\lambda_2 - \lambda_1} N_1^o (e^{-\lambda_1 t} - e^{-\lambda_2 t}) .$$

The activity of the daughter is then

$$A_2 = C_2 \lambda_2 N_2 = \frac{C_2 \lambda_2 \lambda_1}{\lambda_2 - \lambda_1} N_1^o (e^{-\lambda_1 t} - e^{-\lambda_2 t}) ,$$

where C_2 is the counting efficiency of the daughter. Since the time interval between successive chemical separations is held constant, the exponential terms become a constant factor, and A_2 is proportional to the disintegration rate ($\lambda_1 N_1^o$) of the parent at the beginning of each growth period. Thus, if one plots the logarithm of the initial activity of each daughter fraction against the time of

separation, the slope of the line will correspond to the half-life of the parent.

Although the primary emphasis in this work has been on the radiochemical analysis, examination of the gamma ray spectra of some of these neutron-deficient nuclides has also been made with a sodium iodide (thallium activated) scintillation spectrometer coupled to a 50-channel differential analyzer. These gamma ray data are far from definitive, but they have been helpful in the identification of the various nuclides encountered, both new and old. Some of these data will be quoted here when they appear to provide relevant information.

III. RADIOCHEMICAL RESULTS

Figure 1 is a segment of an isotopic chart in the noble metal region showing the activities identified in the present study. The half-lives of previously reported activities are also given in parentheses.

The following is a summary of the experimental results given by mass number.

A = 191. Genetics. --Following a 120-Mev proton irradiation of gold metal, a pure mercury fraction was prepared. The decay curve of the mercury fraction itself was complex, with at least five components. Therefore, a series of seven timed gold separations was made from this fraction at intervals of eight minutes. These gold

milkings showed the activities and genetic relationships illustrated in Table I and Fig. 2.

Table I

Activity	Half-life of Hg parent (or ancestor)(min)	Assignment
40 ± 10 min	20 ± 10	Au^{189}
3.0 ± 0.5 hr	55 ± 10	Au^{191}
15 hr (weak)	>50	Au^{193}
3 d (weak)	~50	Pt^{191}

The 40-minute gold activity is Au^{189}, and will be discussed under that mass number. The 3-hour and 3-day activities descend from the same mercury ancestor, whose half-life is approximately 50 minutes. Further chemical experiments with this gold milking fraction have identified the 3-hour activity as an isotope of gold and the 3-day activity as platinum, hence probably the daughter of the 3-hour gold. Since Pt^{191} is a fairly well-known 3.0-day activity,[6,7] this chain can be assigned to mass 191.

$$Hg^{191} \xrightarrow{55\ min} Au^{191} \xrightarrow{3\ hr} Pt^{191} \xrightarrow{3.0\ d} Ir^{191} .$$

These results are in agreement with the recent work of Gillon et al.[2] who found in their study of conversion lines from 60-Mev proton bombardments of gold:

$$Hg^{191} \xrightarrow{57\ min} Au^{191} \xrightarrow{\sim 4\ hr} Pt^{191} \xrightarrow{3\ d} Ir^{191} .$$

The genetic relationship between the 3-hour Au^{191} and 3.0-day Pt^{191} was also established independently in two other ways:

(a) Platinum was irradiated with 130-Mev protons, and a pure gold fraction was prepared. Seven timed platinum separations were made at 30-minute intervals, with the results shown in Table II and Fig. 3.

Table II

Pt activity	$T_{1/2}$ of gold parent	Assignment
3 day	2.5 ± 0.5 hr	Pt^{191}
11 ± 1 hr	40 ± 10 min	Pt^{189}
3 ± 0.5 hr	15 - 20 min	Pt^{187}

This experiment indicates a half-life of 2.5 ± 0.5 hours for Au^{191}. The other activities will be discussed under the appropriate mass numbers.

(b) Gold was irradiated with 120-Mev protons, and a pure mercury fraction was separated. This was allowed to stand for about 2 hours, after which a gold separation was made from it. Five milkings of platinum were then made from this gold fraction at 3-hour intervals. The platinum milkings contained largely 3.0-day Pt^{191}, and the yields indicated a half-life of 3.0 ± 0.5 hours for its gold parent.

Moon and Thompson[8] have reported an 18-hour Au^{191} descending from a 12-hour Hg^{191}. No evidence concerning the mercury isotope reported by these workers was found in this study but it can be said that if such a Au^{191} isomer exists, it is not the parent of 3-day Pt^{191} within the limits of detection of the chemical genetic experiments reported here. A small amount of a 17-hour gold activity was observed in one of the gold fractions milked from mercury, but its gamma spectrum was shown to be identical (at 8 percent resolution in a scintillation spectrometer) to that of 17-hour Au^{193} and hence it is most likely Au^{193}.

A = 191. Gamma Ray Spectra. --The gamma spectrum of 3-hour Au^{191} was examined in the scintillation spectrometer with a sample which contained mostly that isotope; one of the spectra is shown in Fig. 4. Gamma rays were seen at 140 ± 20, 300 ± 10, 390 ± 20, 475 ± 20, and 600 ± 20 kev, with intensities (corrected for counting efficiency) relative to the K x-rays of 0.1, 0.6, 0.05, 0.04, and 0.1, respectively. Because of the high intensity of the x-rays at approximately 60 kev, nothing can be said about gamma radiation softer than approximately 100 kev.

In the course of several milking experiments, samples containing essentially pure 3-day Pt^{191} were obtained. Scintillation spectra taken with these samples showed, in addition to the K x-rays, gamma rays at 125 ± 10, 175 ± 10, 265 ± 10, 355 ± 10, 405 ± 10, 445 ± 20, and 530 ± 10 kev. One of these scintillation spectra is reproduced

in Fig. 5. The relative intensities of the 265-, 355-, 405-, 445-, and 530-kev gamma rays as determined from the areas under their photopeaks are 0.2, 1.00, 0.8, 0.2, and 1.7, respectively. The abundances of the 125- and 175-kev gamma ray photopeaks were measured as 0.5 and 0.4 relative to that of the 345-kev gamma ray; however, the background under these peaks is rising sharply and there must also be some contribution from backscattered radiation, so these relative abundances are only estimates.

Swan, Portnoy, and Hill[7] have examined the conversion line spectrum of Pt^{191} and have reported gamma rays at 62, 82, 94, 125, 129, 171, 178, 267, 350, 359, 408, 455, and 537 kev. The present scintillation measurements would of course not resolve the 125-129, 171-178, 350-359 pairs, but otherwise are in agreement with the results of Swan et al. above 100 kev. (The gamma ray spectrum below 100 kev could not be examined because of the overwhelming area of the K x-ray peak.)

A = 189. Genetics. --An approximately 12-hour activity in platinum was first observed in 1950 by Thompson and Rasmussen[9] from 50-Mev proton bombardments of iridium, but a mass assignment was not made at that time. With the aid of J. O. Rasmussen, this activity has now been assigned to Pt^{189} by means of proton excitation function experiments in which its yield from iridium is compared with that of 3.0-day Pt^{191} produced from the (p, 3n) reaction

on Ir^{193}. The excitation experiments were done in the Berkeley 32-Mev proton linear accelerator with a set of stacked iridium and aluminum foils as targets and absorbers. Figure 6 shows the resulting yield curves, which exhibit similar maxima at approximately 28 Mev. On the basis of its production from a (p, 3n) reaction in iridium, the new activity can be only Pt^{189} or an isomer of Pt^{191}. The following is evidence against its assignment to Pt^{191m};

(a) iridium was bombarded with 12-Mev protons in the 60-inch cyclotron, and in the platinum fraction the known 3-day Pt^{191} and 4-day Pt^{193m} which are produced from the (p, n) reaction were observed. The 10-hour activity was not found. This is consistent with its assignment to Pt^{189}, because a (p, 3n) reaction is energetically not possible at this proton energy. (Anticipating the discussion of gamma ray studies of the mass 189 chain, it was also observed in this 12-Mev bombardment that the gamma spectrum of the platinum fraction was identical to the known spectrum of Pt^{191}, and had none of the gamma rays associated with the 10-hour platinum.)

(b) Wilkinson, in his study of platinum isotopes produced by 18-Mev deuteron bombardments of iridium,[6] observed no platinum activity with half-life shorter than that of 3-day Pt^{191}. He should not have been able to detect Pt^{189} because at 18 Mev the yield of the (d, 4n) reaction is quite small.

It is also noted from Fig. 6 that the yield curve for the 3-day component shows two maxima. The small peak at approximately 10 Mev indicates the production of 3-day Pt^{191} from the Ir^{191}(p, n)

reaction and of 4-day Pt^{193m} from the $Ir^{193}(p, n)$ reaction, while the ten fold larger peak at approximately 28 Mev corresponds to the $Ir^{193}(p, 3n)Pt^{191}$ reaction. The 11-hour component shows no peak at approximately 10 Mev as might be expected if it were Pt^{191m}, but it seems to be produced only from the (p, 3n) reaction.

Because of these considerations this activity was assigned to Pt^{189}. The best value for its half-life is 10.5 ± 1 hours.

In the decay curves of the platinum fractions from these 32-Mev proton bombardments of iridium, an 11 ± 1-day activity also appeared in addition to and in comparable yield to 10.5-hour Pt^{189} and 3.0-day Pt^{191}. A similar activity was seen in the decay curves of the iridium fractions (in addition to 75-day Ir^{192}). Attempts were made to establish the parentage of this 11-day activity by the timed separation procedure described above, but these were not successful because of lack of reproducibility of the iridium-platinum milkings. Accordingly, platinum-iridium separations were performed on the initial platinum fractions after activities shorter than approximately 10 days were no longer detectable, and it was found that an approximately 11-day activity appeared in both the platinum and the iridium fractions. The gamma ray spectra of these activities were studied with the scintillation spectrometer, and were found to be different from each other (dispelling the fear of grossly incomplete chemical separation). The 11-day platinum activity is undoubtedly Pt^{188}; evidence for this will be discussed under A = 188. That the 11-day iridium activity does not belong to the mass 188 chain was

substantiated by showing that it is still produced at the lower proton energy of 25 Mev, whereas Pt^{188} is not seen. This energy should be below the threshold for the (p, 4n) reaction.

There remain three choices for the assignment of this activity: Ir^{191m}, Ir^{189}, or Ir^{190} arising from iridium impurity in the original platinum fractions. The first choice, Ir^{191m}, may probably be ruled out by the recent discovery of 6-second Ir^{191m} by Mihelich et al.[17] and by Naumann and Gerhart,[18] and also by the fact that this activity was searched for following 12-Mev proton bombardments of iridium, with negative results.

The data indicate that the 11-day iridium is Ir^{189}. However, Ir^{190} has also been reported[10, 11] as an 11- to 13-day activity; in some of the milkings of iridium from platinum in which the 11-day iridium is observed, there is also seen a small amount of Ir^{192} which must have entered the original platinum fraction as an impurity. Because Ir^{190} would be present in the same way the possibility cannot be excluded that the 11-day iridium which is observed may be Ir^{190}. However, in the following discussion on the gamma spectra this isotope shall be referred to as Ir^{189}.

Once Pt^{189} has been identified it becomes easier to recognize its Au^{189} parent. This isotope has been produced in several different ways: (a) J. M. Hollander[19] found the following activities in the gold fraction in bombardments of tantalum (Z = 73) with high energy carbon ions in the 60-inch cyclotron: 10 ± 5 minute, 42 ± 5 minute (predominant), approximately 11 hour, and approximately

10 day (weak). The yields were very low in these experiments because of inadequate beam currents, but timed platinum separations from the gold fraction indicated that the 11-hour platinum (189) is the daughter of an approximately 35-minute gold parent activity. (b) Platinum metal was irradiated with 130-Mev protons, and a gold chemical fraction isolated. Timed milkings of platinum from this fraction (done in separate experiments at intervals of 10 minutes and 30 minutes, respectively) verified that 11-hour Pt^{189} has a gold parent of 40 ± 10-minute half-life. The yield curves from these milking experiments are shown in Figs. 3 and 14.

These experiments demonstrate that Au^{189} has a half-life of 42 ± 5 minutes.

In the experiment discussed under A = 191 (the results of which are given in Table I and Fig. 2), it was seen that the 40-minute gold activity grew from an approximately 20-minute mercury parent. The experiments cited here which establish the 42-minute gold as Au^{189} therefore also set the half-life of Hg^{189} as approximately 20 minutes. This Hg^{189} half-life, however, is the result of only one experiment, so a considerable uncertainty is attached to this value.

The mass 189 chain, insofar as it has been studied can be written as:

$$Hg^{189} \xrightarrow{\sim 20 \text{ min}} Au^{189} \xrightarrow{42 \text{ min}} Pt^{189} \xrightarrow{10.5 \text{ hr}} Ir^{189} \xrightarrow{10 \text{ d(?)}} Os^{189}.$$

A = 189. Gamma Ray Spectra. --A fairly pure Au^{189} sample was obtained from the carbon ion bombardment of tantalum. Gamma ray spectra taken during the first few hours of its decay show, in addition to x-rays, a very prominent gamma ray at 290 ± 10 kev, decaying with the approximately 40-minute half-life of Au^{189} (see Fig. 7). A gamma ray is also seen at 135 ± 10 kev in about 10 percent of the intensity of the 290-kev gamma ray. High energy radiations (>800 kev) may also be present.

The Pt^{189} gamma ray spectrum indicates a fairly certain photon at 140 ± 10 kev, with probable gamma radiation at approximately 550 kev, slightly greater than 550 kev, and at approximately 700 kev.

Bombardments of iridium with 32-Mev protons produce in the platinum fraction active isotopes of masses 193, 191, 189, and 188. If one allows this fraction to decay for several weeks and then removes iridium from it, good samples of Ir^{189} and Ir^{188} are obtained, because Pt^{191} and Pt^{193m} have no active iridium daughters. The 11-day Ir^{189} can be distinguished from 41-hour Ir^{188} by virtue of their very different half-lives. In this way the spectrum of Ir^{189} has been obtained (see Fig. 8), which shows a strong gamma ray at 245 ± 10 kev, and perhaps a weak gamma ray at approximately 135 kev (although this may be backscattered 245-kev radiation). No other radiations than x-rays were seen which could be attributed to Ir^{189}.

A = 188. Genetics and Gamma Spectra. --Naumann[12] has reported the synthesis of a new neutron-deficient isotope of platinum, Pt^{188},

with a half-life of 10.3 days. Although the present work was aimed primarily toward the study of new odd-particle chains, it was of interest to examine the 188 chain because of the possibility of confusion of this 10-day Pt^{188} with the 10-day Ir^{189} reported here. (It has already been mentioned under A = 189 that a 10-day activity had been observed in both the platinum and the iridium fractions from 30- to 50-Mev proton bombardments of iridium.)

The Pt^{188}-Ir^{188} pair has been studied in the following way: a proton bombardment of iridium metal was made at 32 Mev, and a platinum fraction chemically separated. This fraction was allowed to stand for about a month, at which time an iridium-platinum separation was performed. This second platinum fraction exhibited an initial growth, and then decayed with a 10.0 ± 0.3-day half-life. Analysis of the growth curve[13] plus direct decay data yields a daughter half-life of 41 ± 4 hours. This curve is shown in Fig. 9.

The evidence for the assignment of the 10-day activity to Pt^{188}, in agreement with Naumann, is the following:

(a) This 10-day platinum has been observed in bombardments of iridium with 32-Mev protons, which is consistent with its production from the reaction $Ir^{191}(p, 4n)Pt^{188}$.

(b) The daughter iridium activity has been assigned by Chu[11] to Ir^{188} on the basis of its production by an (α, 3n) reaction on enriched Re^{187}.

(c) The gamma spectrum studies of the 41-hour iridium (described below) show that the energies of the first two excited states

in osmium which are populated by its decay are the same as those produced from the beta decay of Re^{188}. This is fairly convincing evidence for its assignment to Ir^{188}.

The gamma spectra of Pt^{188}, Ir^{188}, and of the Pt^{188}-Ir^{188} equilibrium mixture are shown in Figs. 10, 11, and 12, respectively. Gamma rays are seen in Pt^{188} at 195 ± 10, 275 ± 15 kev, and there is a broad peak at approximately 400 kev which may represent two unresolved gamma rays. The measured relative abundances are 1.0, 0.1, and 0.3, respectively. As the Ir^{188} grows into the sample, gamma rays appear at 150 ± 10, 475 ± 10, and 625 ± 15 kev. The relative intensities were measured directly in the second iridium fraction which contains Ir^{188} plus a small fraction of Ir^{189} activity. From the pure Ir^{188} spectrum (Fig. 11) relative intensities 0.9, 0.6, and 1.0 for the three gamma rays, respectively were obtained. There also seems to be harder gamma radiation in low intensity.

Richmond, Grant, and Rose[14] have studied the beta decay of Re^{188} (which leads to the same daughter nucleus as does the electron capture decay of Ir^{188}) and have observed gamma rays of 152, 476, 638, 933, and ~1300 kev. The first three are in good agreement with the gamma rays observed from the decay of Ir^{188}; no comparison with the two high energy gamma rays of Re^{188} can be made other than to say that if the 933-kev gamma ray is present in the decay of Ir^{188} its intensity is less than one-third that of the 625-kev gamma ray.

In two 130-Mev proton bombardments where platinum was milked from a gold parent fraction, preliminary evidence was obtained that the half-life of Au^{188} is of the order of 10 minutes. No further data concerning Au^{188} was produced.

The genetic data on the mass 188 chain are summarized as:

$$Au^{188} \xrightarrow{\sim 10 \text{ min}} Pt^{188} \xrightarrow{10.0 \text{ d}} Ir^{188} \xrightarrow{41 \text{ hr}} Os^{188} .$$

A = 187. Genetics and Gamma Spectra. --An 11.8-hour iridium isotope was discovered by Chu[11] and assigned by him to Ir^{187} on the basis of its production from an (α, 2n) reaction upon Re^{185}. The shape of the excitation curve which he presents (as (α, 2n) plus small contribution from (α, 4n)) is not convincing, however, especially in view of the fact that others have been unable to detect an (α, 4n) reaction with 38-Mev alpha particles in the 60-inch cyclotron. Although the genetic data given here neither prove nor disprove this mass asignment, but only establish the gold and platinum activities which are isobaric with the 12-hour iridium, this reference activity shall be specified here as Ir^{187}. It will be seen, however, that the gamma ray data tend to support this assignment.

Pt^{187} has been identified in the following way: iridium metal was bombarded with 120-Mev protons and a pure platinum fraction chemically separated. (Its decay curve was complex, with components of 2.5 hours, ~10 hours, ~2.2 days, and ~10 days.) After allowing this platinum fraction to stand for one day, iridium was separated from it. This first iridium milking contained largely

14 ± 1 hour (Ir^{187}) and 43 ± 4 hour (Ir^{188}) activities, with a ratio (in counts per minute) of Ir^{187}/Ir^{188} of 6.5. The same platinum fraction was then allowed to stand for an additional day, and iridium was again removed. The ratio (in counts per minute) of Ir^{187}/Ir^{188} present in this second milking was much lower, approximately 0.2. Because Ir^{188} grows from a relatively long-lived parent (10-day Pt^{188}), its actual yield during the two intervals of growth is roughly constant and hence the ratio of Ir^{187}/Ir^{188} in the two milkings gives some idea of the half-life of the parent of Ir^{187}. By the factor of approximately 32 decrease in Ir^{187} in 24 hours, one would say that the half-life of its parent is approximately 5 hours. A possible error would arise from a small amount of 10-hour Pt^{189} impurity in the iridium milkings, which would cause the half-life of Pt^{187} to appear too long. The experiment, then, indicates that the half-life of Pt^{187} is ≤ 5 hours, and probably is the 2.5-hour platinum seen in the original platinum fraction.

Several other genetic experiments were done to identify the mass 187 chain. On two occasions, platinum metal was irradiated with 130-Mev protons, and pure gold fractions prepared. As was expected, the gold fraction decay curves were complex, with at least five components. Therefore, timed platinum milkings were made in each experiment. The results of these milkings are given in Table III, and some of the yield curves are shown in Figs. 13 and 14.

The genetic data on the mass 187 chain are summarized as:

$$Au^{187} \xrightarrow{\sim 15\ min} Pt^{187} \xrightarrow{2.5\ hr} Ir^{187} \xrightarrow{14\ hr} Os^{187}.$$

The only reasonably good gamma ray data at mass 187 were obtained with 14-hour Ir^{187}. Three gamma rays are seen, at 135 ± 10, 300 ± 10, and 435 ± 15 kev, with relative intensities respectively 1.0, 1.1, 0.8. Weak gamma rays are also seen at ~500 kev and at ~ 625 kev, but these may belong in part to Ir^{188}. This spectrum is shown in Fig. 15.

Table III

Activity (hr)	Half-life of gold parent or ancestor (min)	Assignment
Experiment A--five milkings at 7-minute intervals		
2.5± 0.5	~13	Pt^{187}
12 ± 2	~14	Ir^{187}
Experiment B--8 milkings at 10-minute intervals		
3 ± 0.5	~17	Pt^{187}
12 ± 2	~12 (plus ~40)	Ir^{187}(plus Pt^{189})

One further remark may be made about the assignment of this chain to mass 187. In two bombardments of iridium with 32-Mev protons where fast chemistry was done, the 2.5-hour platinum

activity has not been observed, whereas Pt^{188}, Pt^{189} and heavier platinum isotopes are all found. This was interpreted as evidence that this isotope has a mass lighter than 188, since it is produced from high energy proton bombardments of iridium. Yet it could not be lighter than 186, or Chu[11] could not have produced it from an (α, 3n) reaction on Re^{185}. Of the two remaining choices, mass 186 or 187, the gamma ray data on the 14-hour iridium daughter indicates that this isotope has mass 187. The first two excited states of the even-even nucleus Os^{186}, defined by the beta decay of Re^{186}, are at 137 and 764 kev,[15,16] with gamma rays observed at 137, 627, and 764 kev. The principal gamma rays which were observed in the decay of the 14-hour iridium, however, are at 135, 300, and 435 kev. These do not fit into the Os^{186} level pattern, whereas in the case of mass 188, the gamma ray energies which were observed in the decay of Ir^{188} agree quite well with those found[14] from the beta decay of Re^{188}.

After a 50-Mev proton bombardment of iridium a pure platinum fraction was separated and then allowed to decay for 8 days. At this time an iridium milking was made and the following activities were observed: 42 ± 4 hours, 9.5 ± 1 days, and ~~180 days (weak). The 42-hour activity has been assigned by Chu[11] to Ir^{188}, and this work has verified the assignment. The 9.5-day activity has been designated as Ir^{189}. No prior indication of a 180-day activity was seen in this work, but Chu[11] did observe in low abundance an activity of >100 days which he tentatively assigned to Ir^{189}. The

amount of 180-day activity extrapolated back to time of milking was only ~1 percent of the 42-hour activity so there is the possibility that the platinum parent fraction contained some impurity that was removed with the iridium milking.

In the gamma spectrum of this iridium milking there were peaks at 245 ± 10, 200 ± 10, ~130, and ~~335 kev (very weak). The 245-kev gamma ray decayed with an ~12 day half-life and it has been assigned to Ir^{189}, as has also the 130-kev gamma ray. The 200-kev gamma ray had not been previously observed; its half-life is ~~40 days. The 335-kev peak was of such low intensity that no half-half could be determined. The gamma rays of Ir^{192} were not in evidence in this milking 75 days after the separation which indicated that there was a relatively small amount of iridium impurity in the original platinum fraction. The very low abundance of the 200- and 335-kev gamma rays makes it impossible to discount the possibility that they are due to an impurity. No attempt was made to assign these gamma rays to any of the activities observed in this work.

Other Activities. -- One bombardment of 150-Mev alpha particles on rhenium metal was made. The target material was dissolved in 3 ml concentrated HNO_3. Iridium carrier was added and the solution evaporated to dryness to expel OsO_4. The residue was taken up with 3 ml water and 5 ml concentrated formic acid. This solution was heated in a boiling water bath to precipitate iridium. The iridium precipitate was washed with water and plated for counting.

The Geiger counter decay curve could be resolved in the following components: 19 ± 4 minutes, 2.8 ± 0.4 hours, 11.5 ± 1.5 hours, 41 ± 5 hours, 11 ± 2 days, 75 ± 10 days. This was the only experiment where the 19-minute and 2.8-hour activities were observed. Chu[11] has assigned a 3.2-hour activity for Ir^{190} on the basis of excitation functions of alpha particles on natural and enriched rhenium. He reported that this isotope decays primarily by positron emission.

The gamma data obtained from this bombardment were not conclusive but they may be of some value in assigning the various activities observed in the Geiger counter decay. No gamma counts were taken on this sample until 1.5 hours after the end of the bombardment and at this time no radiation between 100 and 800 kev was observed which could be attributed to a 19-minute half-life decay. However, the initial decay of the x-rays gave a half-life of approximately 30 minutes which is in reasonable agreement with the Geiger counter decay when the uncertainties of both measurements are considered.

There was a 115 ± 10 kev gamma ray in the spectra which decayed with a half-life of approximately 2 hours. There was no other radiation <800 kev with a similar decay. There also appeared to be an approximately 3-hour half-life component in the x-ray decay curve. On the basis of half-life considerations alone one might think that the 2.8-hour activity is Ir^{186}. However, Koerts[16] has observed in the β^- branching decay of Re^{186} to Os^{186} that the

first excited state is 137 kev above the ground state. This indicates that the 115-kev gamma ray observed in this work is not the decay of the first-excited state in Os^{186}, therefore the 2.8-hour activity probably is not Ir^{186}. In addition, since no annihilation radiation was observed it appears that the 2.8-hour activity observed in this work and the 3.2-hour positron emitter reported by Chu are not the same activity. No further data on these two short-lived iridium activities were obtained.

IV. REFERENCES, Part I

1. de Shalit, Huber, and Schneider, Helv. Phys. Acta 25, 279 (1952).
2. Gillon, Gopalakrishnan, deShalit, and Mihelich, Phys. Rev. 93, 124 (1954).
3. J. W. Mihelich and A. deShalit, Phys. Rev. 93, 135 (1954).
4. H. Neumann and I. Perlman, Phys. Rev. 78, 191 (1950).
5. D. G. Karraker and D. H. Templeton, Phys. Rev. 80, 646 (1950).
6. G. Wilkinson, Phys. Rev. 75, 1019 (1949).
7. J. B. Swan, W. M. Portnoy, and R. D. Hill, Phys. Rev. 90, 257 (1953).
8. J. H. Moon and A. L. Thompson, private communication (October 1952).
9. S. G. Thompson and J. O. Rasmussen, unpublished data (1950).
10. L. J. Goodman and M. L. Pool, Phys. Rev. 71, 288 (1947).
11. T. C. Chu, Phys. Rev. 79, 582 (1950).
12. R. A. Naumann, Phys. Rev. 96, 90 (1954).
13. The total amount of activity at time t can be expressed as

$$A = \sum_i a_i e^{-\lambda_i t} ,$$

where the a_i's can be either positive or negative. To resolve this growth and decay curve, the "tail" was extrapolated back to the time of purification of the parent and subtracted from the observed curve. The series of negative differences, when plotted, gives the half-life of the daughter.

14. Richmond, Grant, and Rose, Proc. Phys. Soc. (London) 65A, 484 (1952).

15. F. R. Metzger and R. D. Hill, Phys. Rev. 82, 646 (1951).

16. L. Koerts, Phys. Rev. 95, 1358 (1954).

17. J. W. Mihelich, M. McKeown, and M. Goldhaber, Phys. Rev. 96, 1450 (1954).

18. R. A. Naumann and J. B. Gerhart, Phys. Rev. 96, 1452 (1954).

19. J. M. Hollander, unpublished data (1954).

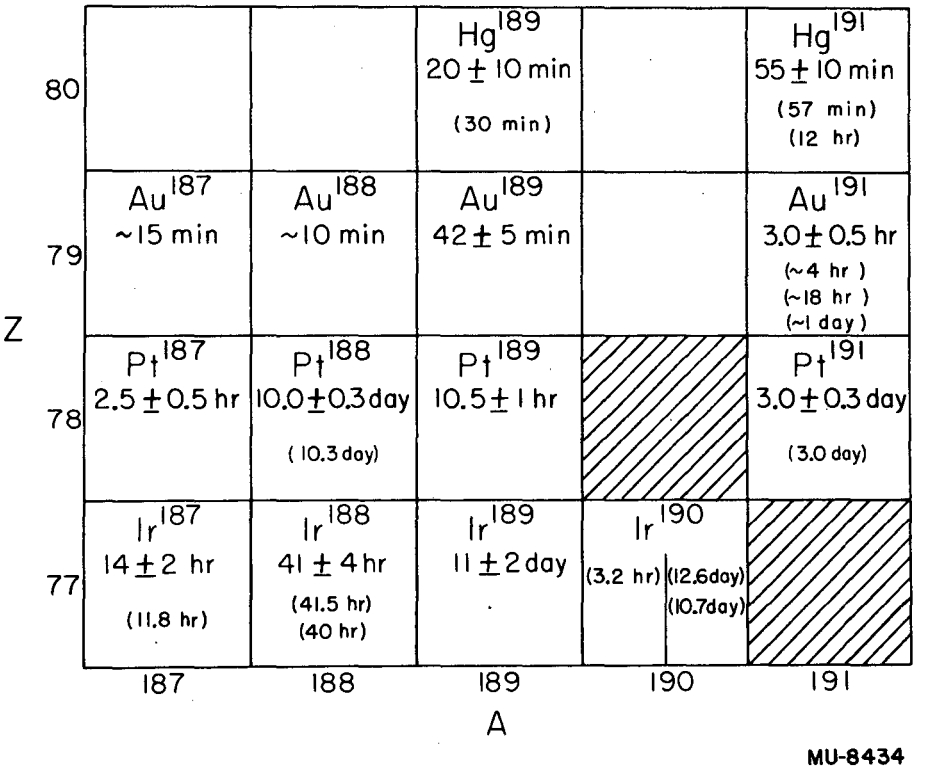

Fig. 1. Segment of an isotopic chart in the noble element region (half-lives in parentheses are previously reported values).

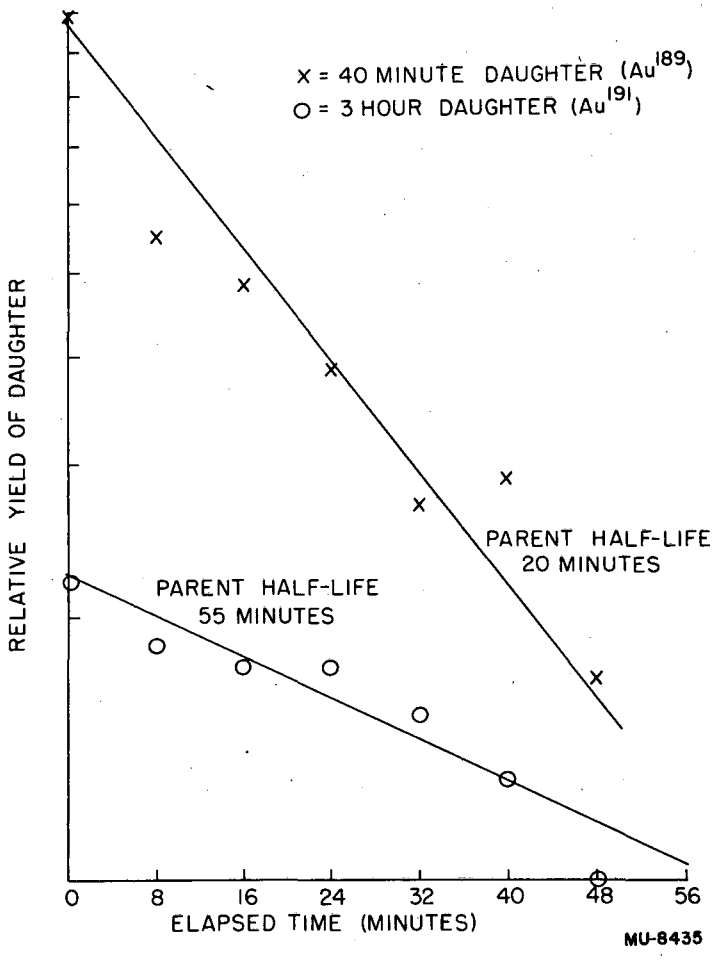

Fig. 2. Radiochemical yield of daughter activities as a function of time. Gold separated from parent mercury fraction at 8-minute intervals. (Bombardment: gold + 120-Mev protons.)

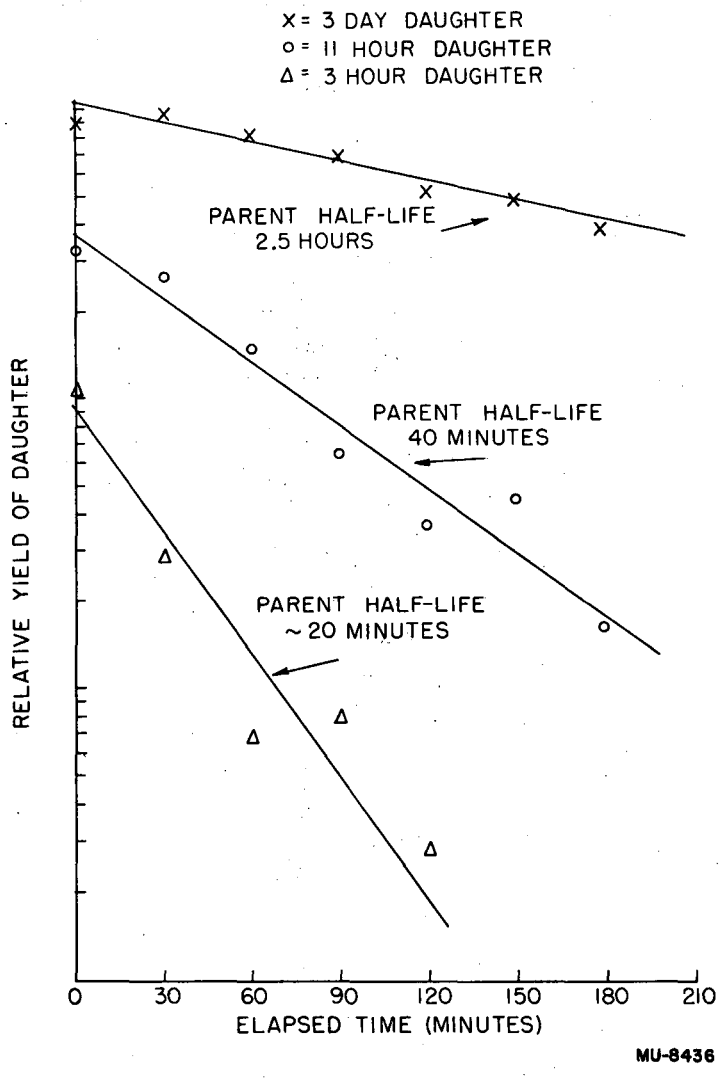

Fig. 3. Radiochemical yield of daughter activities as a function of time. Platinum separated from parent gold fraction at 30-minute intervals. (Bombardment: Platinum + 130-Mev protons.)

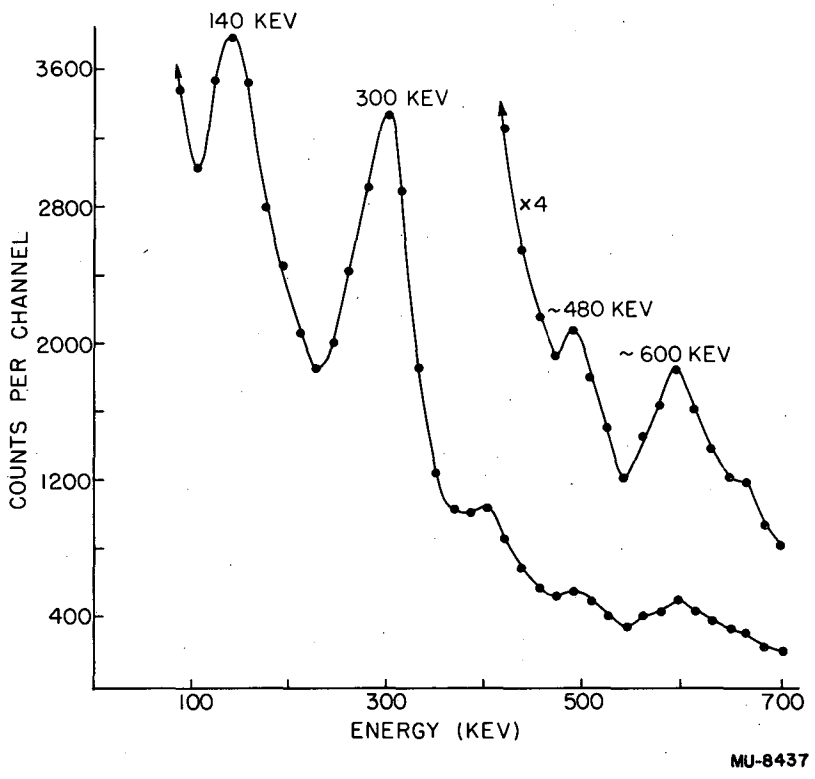

Fig. 4. Gamma-ray spectrum of Au^{191}.

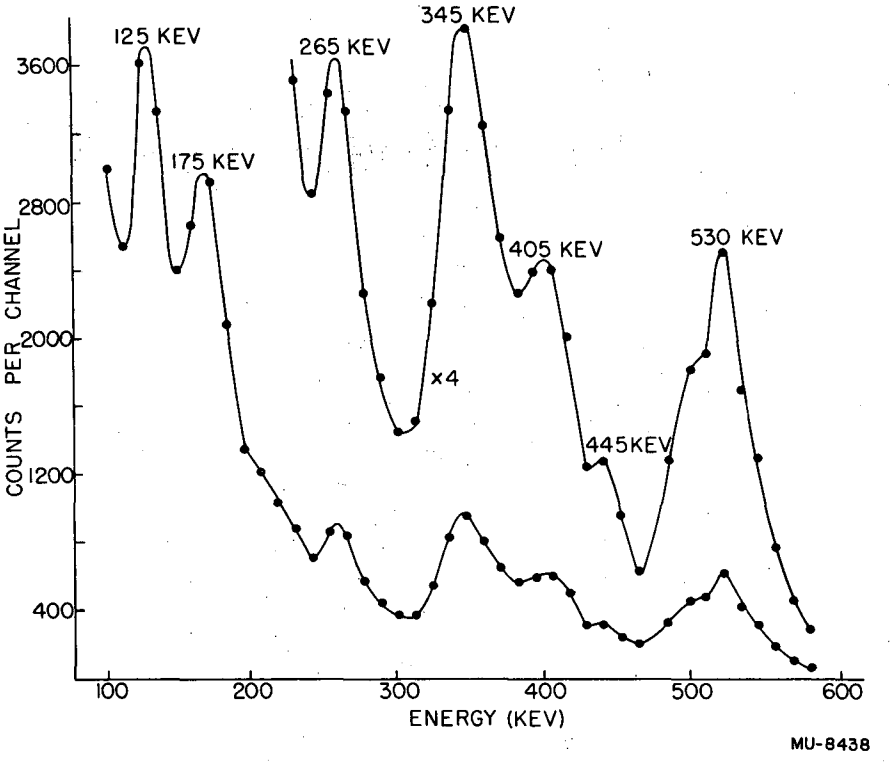

Fig. 5. Gamma-ray spectrum of Pt^{191}.

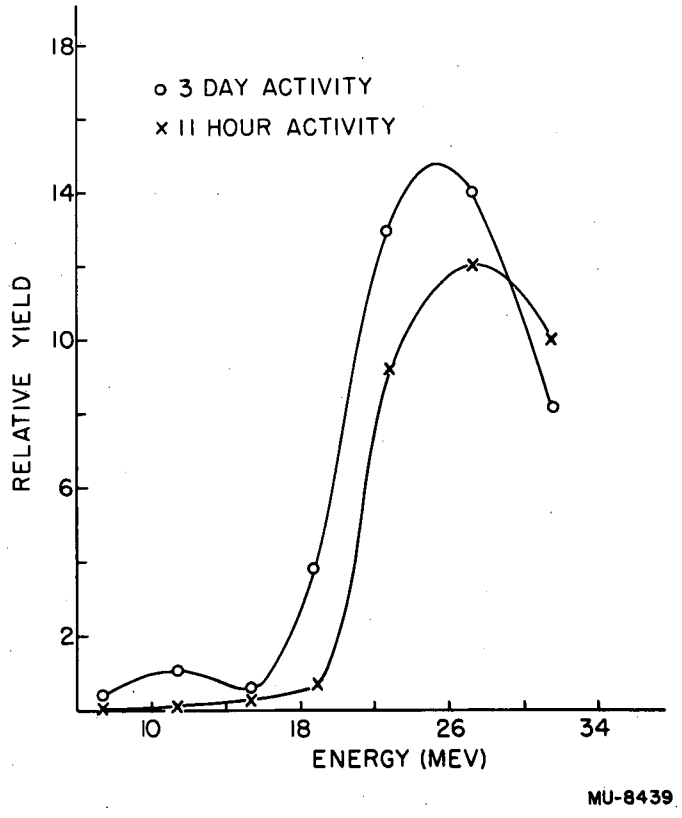

Fig. 6. Excitation curves for the production of 3-day Pt^{191} and 10-hour Pt^{189}.

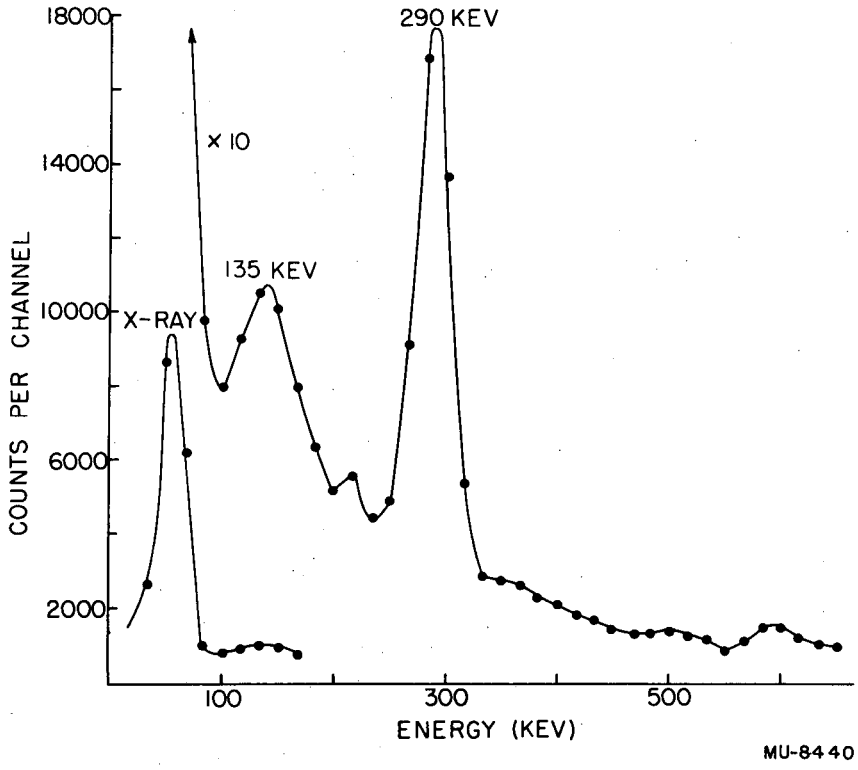

Fig. 7. Gamma-ray spectrum of Au^{189}.

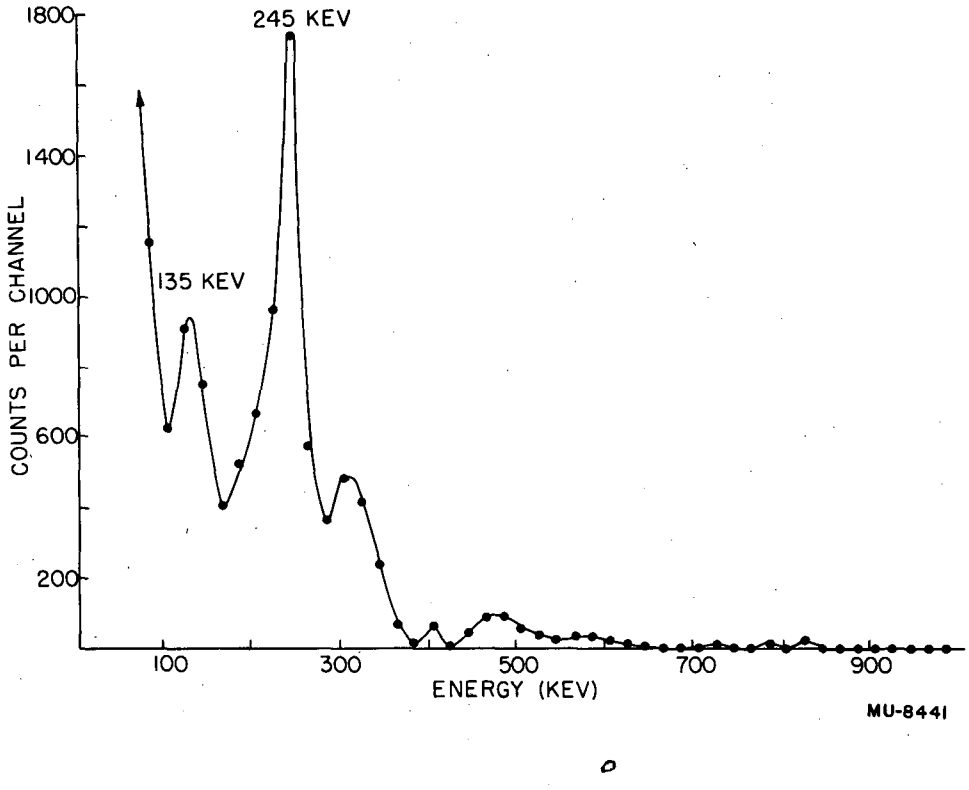

Fig. 8. Gamma-ray spectrum of Ir^{189}.

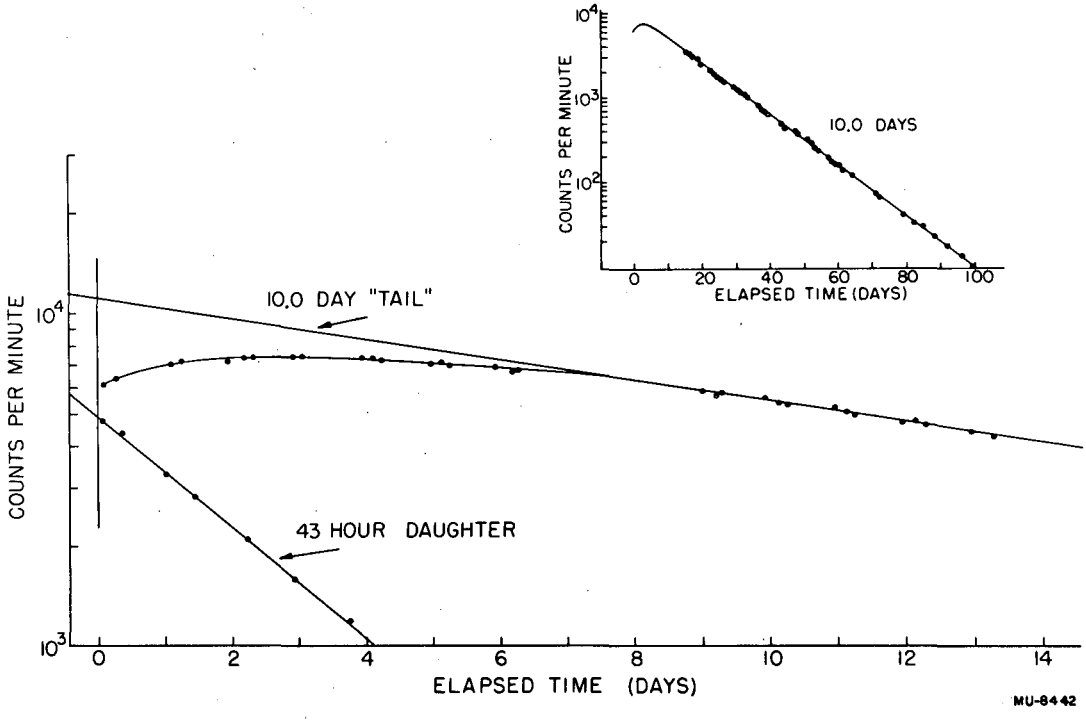

Fig. 9. Growth and decay curve for Pt^{188}, as daughter Ir^{188} grows into equilibrium with parent.

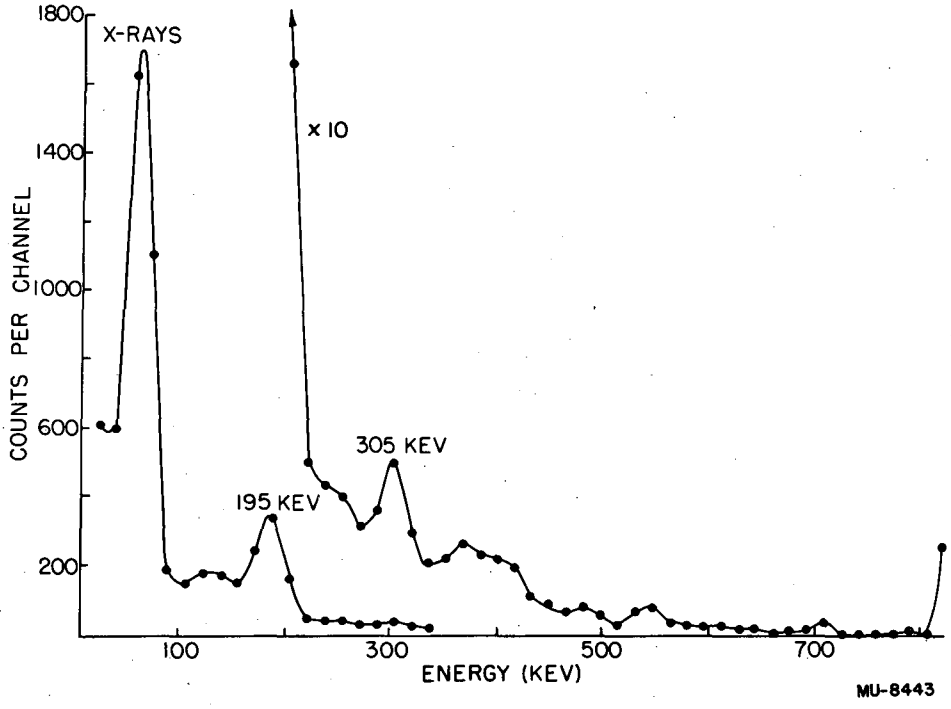

Fig. 10. Gamma-ray spectrum of Pt^{188}.

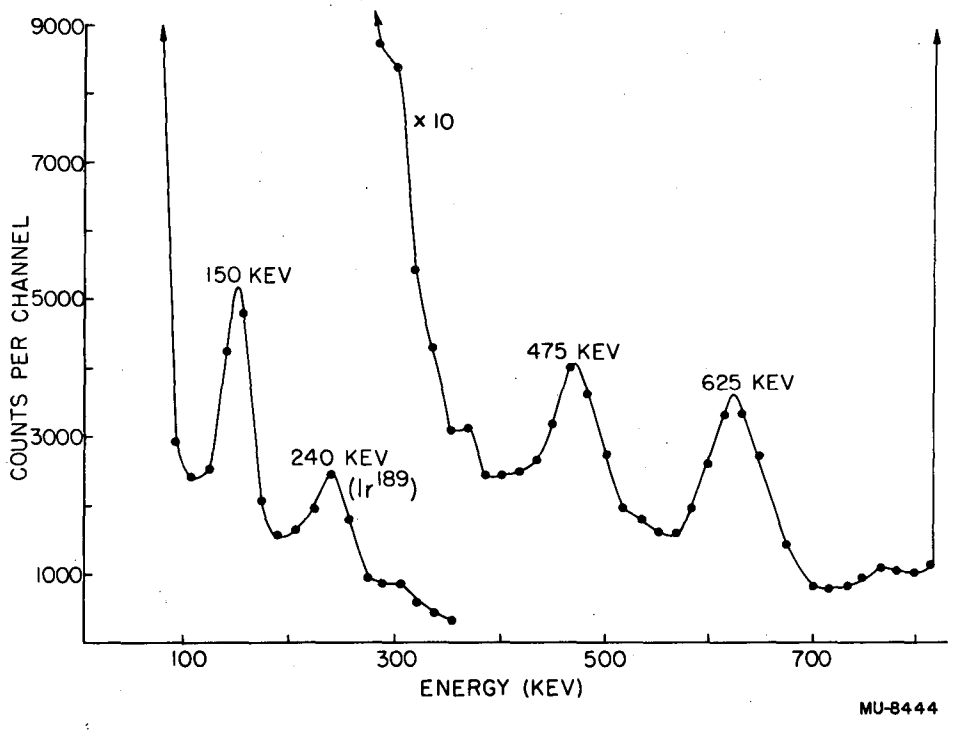

Fig. 11. Gamma-ray spectrum of Ir^{188}.

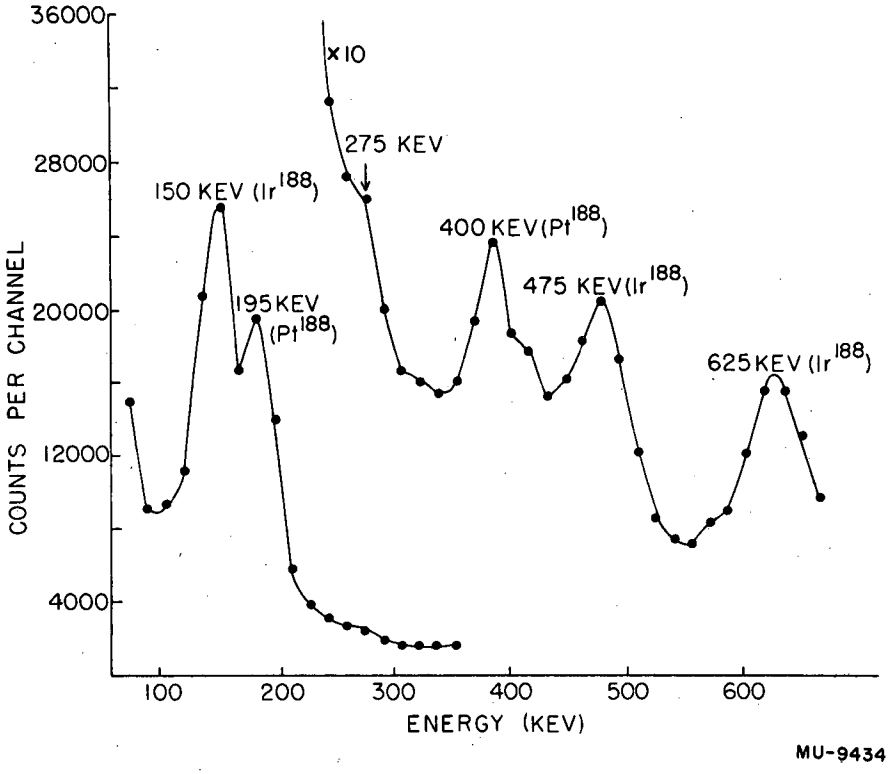

Fig. 12. Gamma-ray spectrum of Pt^{188} in equilibrium with Ir^{188}.

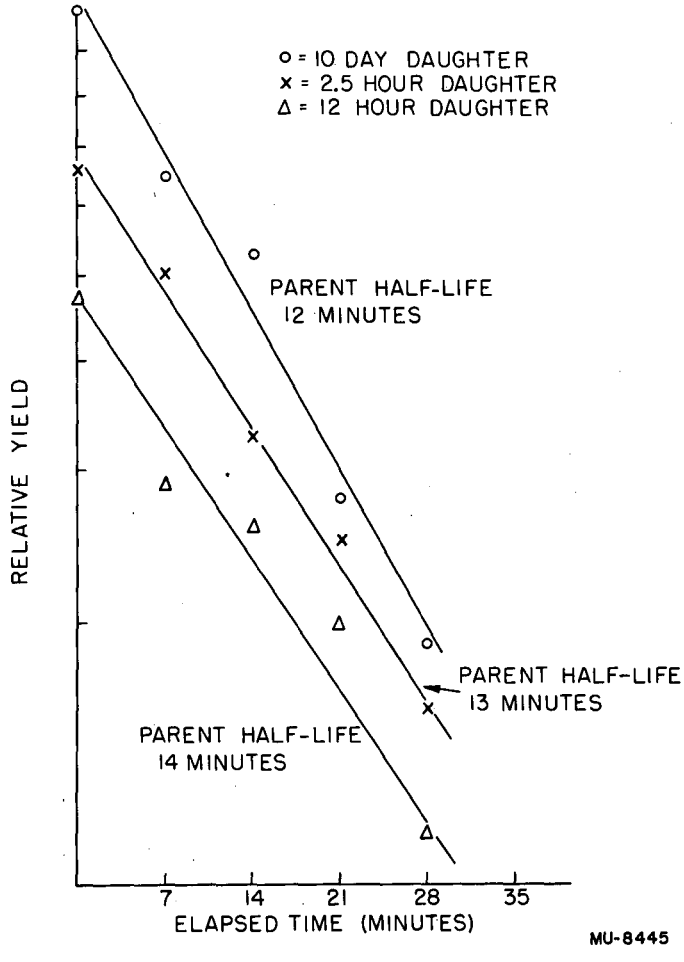

Fig. 13. Radiochemical yield of daughter activities as a function of time. Platinum separated from parent gold fraction at 7-minute intervals. (Bombardment: platinum + 130-Mev protons.)

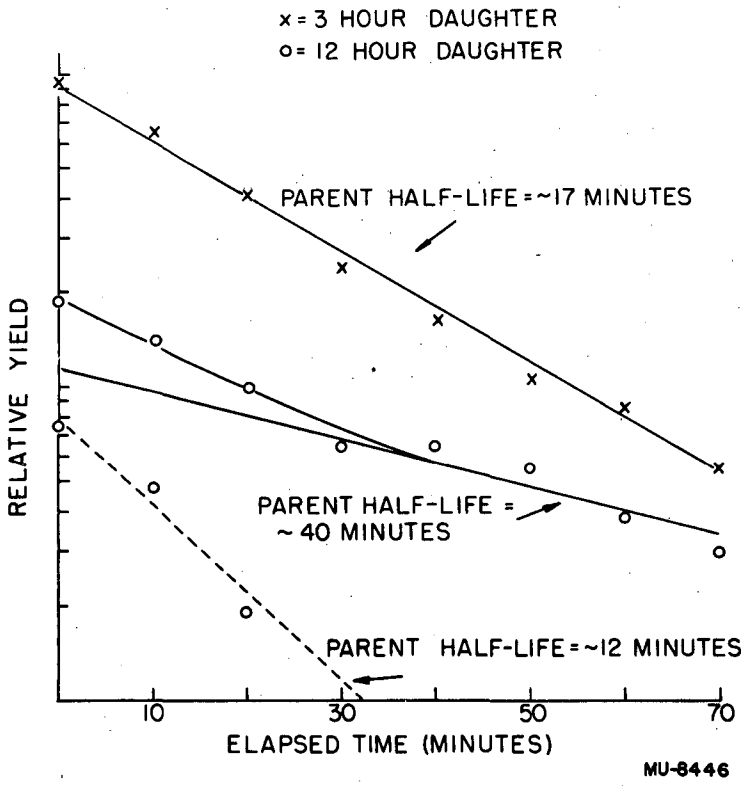

Fig. 14. Radiochemical yield of daughter activities as a function of time. Platinum separated from parent gold fraction at 10-minute intervals. (Bombardment: platinum + 130-Mev protons.)

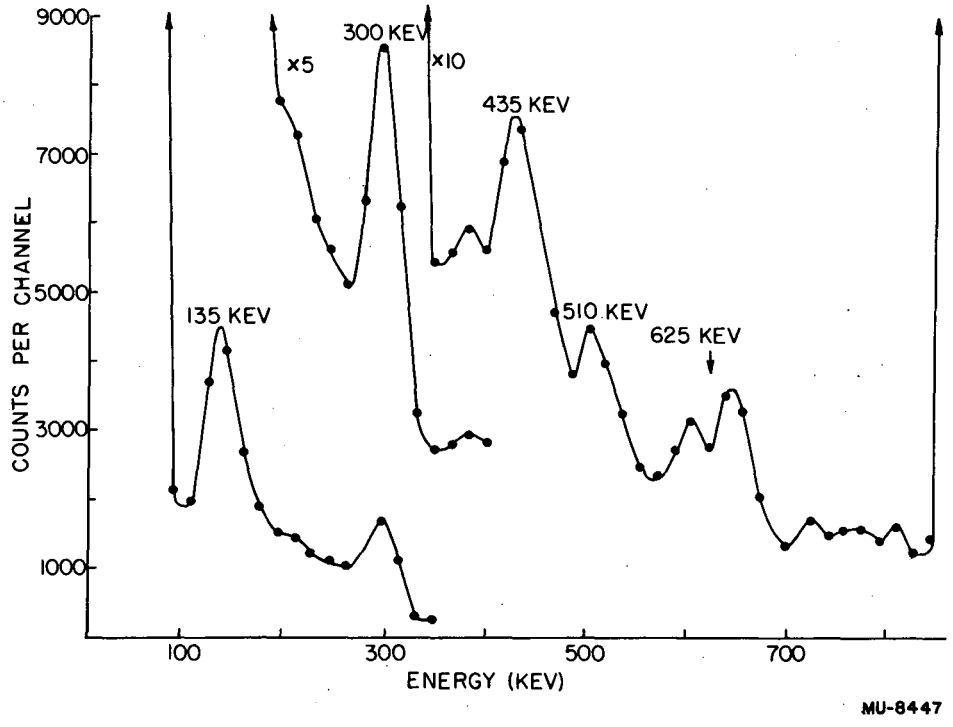

Fig. 15. Gamma-ray spectrum of Ir^{187}.

Part II

I. INTRODUCTION

Nuclear models have arisen from the observation of systematic behavior of various nuclear properties. It has long been realized in the study of nuclear physics that there is a vast difference in the nuclear properties of even-even, odd-even, and odd-odd nuclei, consequently one looks for systematic behavior in similar type nuclei. It is in the study of the different properties where nuclear spectroscopy is valuable.

The shell model[1, 2] arose from the observation of regularities among the spins and magnetic moments of nuclear ground and isomeric states. This extreme single particle model was very successful in explaining some nuclear properties, namely, the spins and to some extent the magnetic moments of nearly all odd mass and odd-odd nuclei. The following assumptions are made in this model: (1) strong spin orbit coupling leading to inverted doublets, predicting that the $(\ell + 1/2)$ state will lie at a lower energy level than the $(\ell - 1/2)$ state, (2) an even number of identical nucleons will couple to give zero angular momentum, indicating that the spins of even-even nuclei will be zero, (3) an odd number of identical nucleons will couple to give the angular momentum of the single odd particle such that the spin of an odd-even nucleus, for instance, will be the spin of the odd proton, and (4) the pairing energy is negative and increases with the ℓ value of the orbit.

This model, however, did not give a good explanation for the magnitudes of some magnetic moments and it gave no information in regard to the magnitudes of quadrupole moments. Two different models have been developed in attempts to explain these properties. Flowers[3] has proposed a model which considers all particles outside the core of completed levels on an equal footing. The calculations have been made for the magnetic moments of a number of odd-mass light nuclei and better agreement with the experimental values is obtained than is obtained with the extreme single particle model. The Flowers model also describes how electric quadrupole moments arise in odd-neutron nuclei without the assumption of a deformable core.

The other model which attempts to give a more complete explanation of nucleon properties than does the single particle was proposed by Bohr and Mottelson.[4] This model takes into account the collective motion of nucleons and is particularly successful in its application in regions far removed from closed shells, so-called strong coupling regions. The unified nuclear model attempts to predict, with a fair measure of success, spins, quadrupole moments, magnetic moments, nucleon level structure, and transition probabilities.

This very brief description of some of the current nuclear models was cited to illustrate the usefulness of the data obtained in nuclear spectroscopy in formulating and testing nuclear theory.

It was attempted in the present work to obtain more information on the nuclear properties of the heavy elements. The systematics observed in the alpha decay of the heavy elements were most important in the formulation of Bohr's unified model theory. In addition this region is especially fruitful in contributing data which can be applied to nuclear theory since many of the isotopes can be studied by their beta and/or electron capture decay as well as alpha decay. This was the reason for making the presently described study of conversion electrons with permanent magnet spectrographs.

The high resolution and accuracy of this type of spectrograph makes possible two important types of measurements. First, the conversion electrons of gamma rays with very similar energies can be resolved, which permits the identification of the separate gamma rays and gives accurate energy values. Second, since the electron lines are well resolved, relative intensities of the electrons from different atomic shells can be obtained.

Measurements of these types were carried out in this work. At the present time theoretical calculations have only been carried out to make predictions for the relative conversions in the three L electron shells; however, relative intensity measurements were made not only in the L shell but also in the M shell and some approximate intensities were obtained for the N shell. When possible, the experimental values were compared with the theoretical predictions.

II. THE INSTRUMENTS

Permanent magnet 180° spectrographs have been used for many years[5] but with the advent of variable field spectrometers their popularity greatly decreased. However, there has recently been more interest in the study of low-lying nuclear levels and the application of these studies to nuclear theory and models. One way to obtain information about nuclear levels is to study the conversion electrons emitted when a transition occurs. Permanent magnet spectrographs are well suited to measurements of relative electron conversion and the absolute energies of the electrons since they have high resolution and accuracy. (Persico and Geoffrion[6] have recently made a general theoretical study of various types of beta ray spectroscopes.)

Figure 1 is a schematic drawing of a 180° permanent magnet spectrograph. The conversion electron source is placed at S. The active samples are usually mounted on 5- to 15-mil diameter wires or a foil of approximately the same width. The sources are approximately 1 inch long and are arranged normal to the plane of the diagram. Above the source is a relatively wide slit AB and in a continuation of the plane of the slit is a photographic plate EP. The entire arrangement is contained in a box which can be evacuated and placed between the poles of a magnet so that the magnetic field is perpendicular to the plane of the diagram and uniform over the path of the electrons. Particles of the same velocity will describe circles of the same radius in the uniform magnetic field, and it can

be seen from the diagram that even with a relatively wide slit the circles converge to a focus on the plate. The circle which passes through 0, the foot of the perpendicular from S on the plane ABP, just completes a semicircle and attains the farthest distance along the plate from S, all other circles, whether passing through AB to the right or left of 0, strike the plate nearer to the source. Therefore there is, no matter how wide the slit AB, a definite limit to the line on the side opposite the source, and further, owing to a fortunate property of the geometry of the circle, most of the electrons are concentrated into this edge. The geometrical property of the circle which causes "focusing" of the electrons is: if a circle is given an infinitesimal rotation around one of its points, S, the point diametrically opposed is displaced along the tangent. The high-energy side of the line is thus sharply defined and the momentum of the particles can be determined quite accurately by measurement of the position of this edge. Other monoenergetic electrons will also converge at the photographic plate and give sharp-edged lines in a similar manner, the line due to electrons of higher energy being farther from the slit. The only conditions which it is necessary to observe in the arrangement of the apparatus is that the slit AB should be in the continuation of the plane of the photographic plate and symmetrically disposed about the foot 0 of the perpendicular from S. The radius of curvature p of the path of the electrons giving a particular line is thus given in terms of the lengths g and x by the well-known theorem of geometry:

$$(2p)^2 = g^2 + x^2$$

where g = OS and x is the distance between 0 and the high-energy edge of the line. H·p is called the magnetic rigidity and is constant for an electron of a particular energy. There exist tables of Hp vs electron energy, in kev, from which the electron energy for any given Hp can be found. H has to be determined by separate experimentation.

The double cross-hatched area in the diagram represents a lead absorber which is used to protect the photographic plate from direct exposure to the gamma rays of the source.

There are also baffles in the camera to reduce the scattering of electrons into the film.

Two 180° permanent magnet spectrographs of the Brookhaven type were used in this work. The magnetic fields are approximately 50 gauss and about 100 gauss and the spectrographs are designated PMI and PMII, respectively. Electron energies up to about 85 kev and approximately 275 kev can be recorded in PMI and PMII, respectively. The magnets have pole gaps of 12 x 20 x 2 inches into which the spectrograph "cameras" are inserted. The camera chamber is evacuated to a pressure of approximately 10 μ with a Welch Duo Seal rotary, mechanical pump. Figure 2 shows both magnets with the vacuum pumps located under the bench. The camera is in position in the magnet on the right, the camera chamber is visible in the other magnet.

The cameras were also modeled after the Brookhaven instruments. The two cameras used are not exactly identical in construction. Therefore, they are not interchanged in the magnets, e.g., camera A is used in PMI and camera B is used in PMII; all calibrations, etc., were performed under these conditions. No provisions were made in the cameras for rapid source placement, film removal, etc., because only relatively long-lived isotopes are being studied at the present time.

A full view of one of the cameras with the cover plate removed is shown in Fig. 3. The devices at the upper end of the camera are light-tight valves that are opened by contacting the rear plate of the camera chamber when the camera is inserted into the magnet. These valves permit evacuation of the camera chamber. A close-up of the wire source and collimating slit is shown in Fig. 4. Figure 5 shows a source holder with a source in position and Figure 6 is the film holder and film holder backing plate. The film holder calibration notches are visible in the latter figure.

Eastman No Screen X-ray Film with a 1 μ protective coating has been used for line recording. The protective coating absorbs most electrons with energies less than approximately 10 kev. The emulsion has been especially prepared on 3/4 x 15 x 0.040-inch glass backing.

III. SOURCE PREPARATION

One of the most important requirements for the production of sharp and narrow lines in a 180° spectrograph is a narrow and thin source. In addition, if the sample is on a thin wire, the wire must be straight to achieve optimum results. Source preparation problems are not unique to this type of instrument, but are generally among the most difficult problems in beta spectroscopy.

In order to determine roughly what effect a 0.4-mm diameter wire source would have on the electron energy determination the following calculations were made. The calculations were made for an infinitely thin source located 0.2 mm, the radius of the wire, toward the high-energy end of the film relative to the line normal to the film which goes through the center of the slit and also located 0.2 mm, wire radius, further than the usual source position behind the plane of the film. This is the position of the point, in a plane parallel to the bottom of the camera, which is furthest toward the high-energy end of the film. (These calculations pertain, in part, to a case of source misalignment.) No attempt was made to take into consideration electron paths which were not parallel to the camera bottom, only two dimensions being considered. The calculations were made for electron radii of 20, 10, and 5 cm.

At p = 20 cm:

The energy error due to misalignment parallel to the film will be considered first. The source, and consequently the electron lines,

will be shifted in the direction of higher energy. The effect is to give an energy 0.10 percent higher than the real energy. The effect of being further behind the film plane is to give a lower energy; in this case 0.01 percent too low. Adding the two effects gives an energy that is 0.09 percent too high.

At p = 10 cm:	
First effect - energy	0.19 percent high
2nd " - "	0.04 percent low
Sum " - "	0.15 percent high

At p = 5 cm:	
First effect - energy	0.35 percent high
2nd " - "	0.16 percent low
Sum " - "	0.19 percent high.

A comparison of electron lines produced by different type sources can be made by observing the plate reproductions shown in Fig. 7. The upper one was produced from a mixture of Cm^{242} and Cm^{244} vaporized on 2-mil aluminum foil, the width being about 3 mm. The lower is from a Cm^{242} sample electrodeposited on a 14-mil platinum wire. (The physical arrangement of the camera was changed slightly between the two runs, therefore all of the lines of Cm^{242} do not exactly coincide.) The vaporized sample should be better from the standpoint of thickness which makes the improvement due to the use of the wire source even more striking.

The very broad lines on the Tm^{170} plate reproduction shown in Fig. 8 are the result of a wide source, approximately 3 mm, and a large slit width. (This film was on cellulose backing.)

The energy error due to using a source wire of finite dimensions is not as serious as it first appears since the spectrographs were calibrated by using standards on wires with approximately the same diameters as the wires on which the samples were mounted. In addition the activity is uniformly distributed on the wire which would tend to mitigate the above effect. The electron line shape[7] is such that an extrapolation to zero blackening should not be made when the line position is determined with the comparator, the initial heavy blackening should be used in this measurement. It was decided on the basis of previous experience and the early part of this work to mount samples on wires whenever possible. It was with this in mind that the following procedures were developed.

The actinide samples used in this work were plated on 10- or 15-mil platinum wires by the electrodeposition process suggested by Harvey.[8] In this method $M(OH)_3$, where M is any actinide, is deposited on the cathode of an electrolysis cell using ammonium bisulfate at a pH of 3.6 as the electrolyte. This plating solution is prepared by bubbling NH_3 gas into a 0.1 $\underline{M}$ H_2SO_4 solution until the pH reaches 3.6.

The cell type used by Harvey was modified in order to plate the activity on a straight wire. The cell wall was formed from 10-mil platinum foil. The foil was wrapped around a quartz rod 0.5 cm in diameter with approximately 3/16 inch of overlap and with a length of about 2.5 inches. The overlapped joint was heated to red color

and sealed by pressing together with another quartz rod. The platinum cylinder was then removed from the quartz rod and a short 30-mil platinum wire was spot-welded to one end for connecting to the cell power supply.

A lucite plug was machined so that it would just slip into the cylinder 0.25 inch, a 40-mil hold 3/8 inch deep hole was drilled into the plug from the end that was placed in the cylinder, and it was glued in the cylinder with Duco cement. A Teflon guide was machined so that it would slide into the cylinder for 1 inch with a loose fit and a 40-mil hole was drilled lengthwise through this plug. (Suitable flats must be machined on the latter plug in order for the gases produced from the water electrolysis to escape.)

To operate the cell, 0.5 ml of plating solution with the actinide activity added was put into the cell with a transfer pipet; this gave a solution depth of 1 inch which is approximately the wire length used in the spectrograph. The Teflon guide was placed in the cell and the sample wire was dropped through the guide hole and into the hole in the lower plug, the hole depth in the latter permitting observation of the wire when it was properly positioned. The sample wire was connected to the cathode of the power supply and the platinum cell wall to the anode. The cell current flow was adjusted to 300 milliamperes per cm^2 of cathode surface, and operated for about 2 hours. At the end of this time the upper guide and the sample wire were quickly removed and 0.1 ml of 6 M NH_4OH added, the guide and wire were replaced and the cell was operated for

10 minutes longer. The NH_4OH is added to prevent the $M(OH)_3$ from dissolving in the acidic plating solution. Another possibility would be to remove the sample wire and quickly place it in a dilute NH_4OH solution but this has not been tried.

After the plating is completed the wire was heated in a methane gas flame to minimize any subsequent loss of the material which usually had a very high alpha specific activity. Approximately 5/16 inch was cut off of the lower end of the wire which had been in the small hole at the bottom of the cell and consequently was relatively free of activity. The other end of the wire was then cut off to give a wire length of approximately 1 1/16 inches.

The ThB source used in calibration was prepared in the following manner. A sample of Th^{228}, approximately 10^9 disintegrations per minute, was deposited on an aluminum plate, and this plate was placed in a lucite box with provisions for making an electrical connection to the plate and for inserting a source wire, also with an electrical connection, to a position about 1/4 inch away from the source. The aluminum plate was attached to the anode and the source wire to the cathode of three 300 volt B batteries connected in series. The half-life of ThB, Pb^{212}, is approximately 10.5 hours, therefore the wire is nearly saturated in 2 days. It is desirable to use as small a volume as possible for the containing box in order to maximize the concentration of Em^{220}.

The I^{131} calibration source was prepared from a fission product iodine solution obtained from the Oak Ridge Laboratory. A 10-mil

silver wire was placed in the solution for 30 minutes to 1 day, the time depending upon the activity level of the iodine solution and the desired source strength. I^{131} deposits chemically on the wire as AgI.

Gray and Stoner[9] prepared samples of At^{211} produced in 60-inch cyclotron bombardments of bismuth with 29-Mev alpha particles. The bismuth target material was melted in a vacuum with a stream of nitrogen present to prevent the gases from condensing on the walls of the apparatus. A cold finger with a thin layer of ice which contained a small amount of perchloric acid was placed in the system and the nitrogen carried the astatine to the finger where it was condensed. The ice layer was melted into a centrifuge cone, an approximately 1 1/16 inch long x 15-mil silver wire was placed in the melt and the solution was stirred for about 1 hour. The astatine was deposited on the wire in a manner thought to be analogous to the preparation of the I^{131} standards.

Stoner and Gray[10] prepared sources of Em^{211} which was produced by the spallation of Th^{232} with 340-Mev protons. The Em^{211} was deposited on 14-mil platinum wires with the use of a glow-discharge tube.[11] (This procedure has been described also by Mathur and Hyde.[12])

IV. INSTRUMENT CALIBRATION

The spectrographs were calibrated by using some of the well-known conversion electron lines of ThB, I^{131}, and Am^{241}. The calibration consisted of the determination of the various radii of

curvature p for the electron lines of the standards, and of the position relative to the source of a series of reference notches on the film holder. (The film holder is shown in Fig. 6.)

The distance from the center of the collimating slit to the nearest reference notch on the film holder ($\underline{B} + \underline{W}$) and the normal distance of the source from the film plane $\underline{g}$ were measured mechanically. A film exposure using ThB which has heavy continuous beta spectra in addition to conversion electrons was made to obtain a plate on which the reference notches were sharply defined. A reproduction of this plate is shown in Fig. 9. The distances between the notches were measured with a travelling microscope, with the total distance from the first reference notch to the notch nearest the electron line defined as Δl_1. When actually determining the position of an electron line the nearest notch in the direction of lower energy was always used. This permitted the addition of all positive distances to obtain the total distance of the line from the center of the slit. The final measurement required was the distance of the high-energy side of the electron line to the nearest reference notch in the direction of lower energy. This distance was measured with a Norelco x-ray film comparator and was defined as $\underline{a}$.

The sum $(B+W+\Delta l_1+a)$ is the distance from the center of the collimating slit to the high-energy edge of the electron line and was previously defined as x. The radius of the electron path p can be calculated using the equation: $(2p)^2 = g^2 + x^2$. The Hp values of the conversion electrons of the standards are accurately known

and this value is divided by the experimentally determined p in order to find the effective magnetic field acting upon an electron traversing a particular path. The effective field is determined at as many values of p as possible and then a plot is made of $H_{eff.}$ vs p. The effective field for any p value of an electron line is obtained from this curve and the energy of the electron is calculated using $H_{eff.} \cdot \rho$.

The film holder reference notches are similar to the type used by Slätis.[13] However, it was found that the thickness of the film holder where the notches were machined, which was approximately 1/8 inch, caused a shadow on the film at the high-energy side of the notch and consequently only the low-energy side was used as a reference point. The shadow effect is especially apparent when the film background is rather light. Slätis[13] did not have this problem with his study of ThB and all of his a measurements were <1 cm; a measurements <2 cm are produced when the reference points are 2 cm apart.

The conversion lines, Hp values used, and references of the calibration standards are in Table I.

These standards were run on one or both spectrographs, p values were determined, and the effective magnetic fields were calculated. In some cases I^{131} and/or ThB was deposited on the wire with the isotope(s) being studied to give energy standards on the same film with the unknown electron lines. These two standards are quite well suited for this purpose since they have fairly short half-lives

Table I

	Line	Hp (gauss-cm)	Reference(s)
ThB	A	534.1	14
	F	1388.5	14, 15
	I	1754.0	14, 15
I^{131}	80.164-K	736.09	16
	80.164-L_I	954.79	16
	80.164-M_I	983.97	16
	80.164-N_I	990.11	16
	284.307-K	1879.91	16
Am^{241}	33.20-L_{II}	365.40	17
	33.20-L_{III}	424.23	17
	33.20-M_I	566.25	17
	33.20-M_{II}	570.25	17
	33.20-M_{III}	579.96	17
	59.57-L_I	661.73	17
	59.57-L_{II}	669.43	17
	59.57-L_{III}	704.08	17
	59.57-M_I	802.36	17
	59.57-M_{II}	805.67	17

and after they have decayed an essentially pure sample of actinide, etc., remains. ThB has a heavy continuous beta spectra background which obscures weak lines of the sample being studied. To minimize the effect of errors introduced into the determination of the effective magnetic field by the use of standards mounted on relatively large wires, approximately the same source diameters were used for unknowns and standards.

To illustrate the reproducibility of the positions of the electron lines, and the field determinations the results of two I^{131} runs on PMII are in Table II.

Table II

	Line	a (cm)	p (cm)	$H_{eff.}$ (gauss)
Run I	80.164-K	0.076	7.431	99.06
	80.164-L_I	0.595	9.636	99.09
	80.164-M_I	1.198	9.932	99.06
	80.164-N_I	to weak to measure		
	284.307-K	1.349	18.924	99.34
Run II	80.164-K	0.074	7.430	99.07
	80.164-L_I	0.595	9.636	99.09
	80.164-M_I	1.180	9.923	99.15
	80.164-N_I	1.330	9.997	99.04
	284.307-K	1.355	18.927	99.36

A discussion of the effects of source misalignment was given in the section on source preparation but it should be noted here that an alignment error of a few mils will cause an error of a few tenths percent in the energy determination. Since the source position is determined mechanically this is undoubtedly the limiting factor in the energy measurements. If very fine, 1- to 2-mil diameter, wires were used for mounting the sources one would surely want a more accurate method to position the source.

Figures 10 and 11 give the calibration results obtained for the two spectrographs. The effective magnetic fields used in the calculations of electron energies were taken from these curves.

The energies of the Auger electrons emitted in the decay of I^{131} were determined from an exposure in PMI. The effective magnetic field of PMII was calculated using these energies and the points are included in Fig. 11. The disagreement with the effective magnetic field calculated from the ThB A line was so large, however, that the Auger electron determined points were not considered in drawing the curve. At the present time there is no explanation for this discrepancy but further calibration will be performed.

The resolution of a beta spectrometer is defined as $\Delta p/p$, where Δp is the width of the electron peak at the point where the electron density is one-half of the maximum density. The resolution of PMI using a source of I^{131} on a 10-mil silver wire is about 0.15 percent. A similar source in PMII gave a resolution of approximately 0.3 percent.

In nearly all cases where conversion electrons from more than one shell were observed for a given transition the energies calculated for the transition from the various groups varied less than 0.1 kev.

The x-ray absorption edge energies of Hill, Church, and Mihelich[18] were used to calculate the transition energies. (Kinetic energy of the electron plus x-ray absorption edge energy equals the transition energy.)

Marchant Table No. 81 was very helpful in calculating the many square roots required in this work.

V. FILM CALIBRATION AND INTENSITY MEASUREMENTS

The problem of determining relative electron line intensities by photographic methods is considerably more difficult than is the determination of the electron energies. Slätis[19] has recently devised a procedure which greatly reduces the amount of work involved in determining the relative intensities and the results are quite accurate. The method used in this work for determining intensities represents a slight modification of Slätis' method.

Until 1927 the only method used to determine relative intensities was by visual estimation. However, in 1927 Ellis and Wooster[20, 21] initiated the method of utilizing the areas under the peaks of the curve obtained from a densitometer trace of a photographic plate. They actually integrated these areas and these integrations were laborious. Slätis' method disposes of this integration.

There are a number of features of the photographic action of electrons that must be studied in order to obtain relative intensities of electron lines.

Ellis and Wooster verified the reciprocity law for heterogeneous electrons. This shows that the photographic density D is the same for all values of P and t when the product (P·t) is held constant. $D = \log I_o/I$, P is the intensity of the electron source in arbitrary units, and t is the time also in arbitrary units.

The photographic blackening as a function of exposure must be experimentally determined for the particular film being used. Ellis and Wooster showed that the shape of the curve obtained by plotting D vs E (exposure) is independent of the energy of the electrons. This was later verified by Dudley.[22] The importance of this independence of the shape of the D-E curve from electron energy cannot be overstressed from a practical standpoint. If the shape was not independent of the energy the experimental curve would have to be obtained for all of the different individual energies of the electrons being studied. However, the shape independence permitted the experimental determination of the D-E curve using a beta-emitter as the source of electrons. This is very helpful since a source can be chosen which emits no gamma rays which would expose the film. If gamma rays are present due to the source, the electron paths could be curved with a magnetic field in a manner such that the film would be exposed only by the electrons, but this necessarily complicates the apparatus required.

The dependence of the line intensity on the radius of curvature of the electron path p must also be determined. Slätis showed that the intensity is inversely proportional to p provided the collimating slit is in the plane of the film.

And finally the photographic blackening as a function of the energy of the electrons must be known. This blackening efficiency for Eastman No Screen X-ray Film which was used in the present work was obtained from two sources. Cranberg and Halpern[23] measured the electron efficiency in the range 9 to 40 kev with the use of an electron gun. Dudley[22] covered the range 35 to 1800 kev using radioactive sources. The slopes of these two curves in the energy region where they overlapped were approximately the same, therefore the curves were normalized and the resultant curve was used for intensity measurements. This curve is shown in Fig. 12.

The D-E relation was determined by a series of Sr^{90}-Y^{90} exposures. A device was made for exposing a portion of a film to a collimated beam of electrons from a Sr^{90}-Y^{90} source. The size of the collimation slit was 1/8 x 1/2 inch and the film was moved approximately 1/2 inch after each exposure. The exposure interval was varied from 2 minutes to 3 hours with approximately 12 exposures per film. All photometer measurements were made with an Applied Research Laboratories densitometer used in conjunction with a Leeds and Northrup Speedomax Recorder.

The density of an electron line is also a function of the time of development. Most of the films in the present work were developed

for 3 minutes but in cases where it was anticipated that the lines would be weak 5-minute development was used. All films were developed at 68° F in full strength Kodak D-19 developer, fixed for 15 minutes in Kodak x-ray fixer, and washed in distilled water for 15 minutes. The results of the D-E experiments are shown in Fig. 13. One strontium-yttrium exposure sequence was developed for 3 minutes and the other for 5 minutes. The results of this experiment are in excellent agreement with the work of Dudley.[22]

Having established the density-exposure, efficiency-energy, and intensity-radius relations it is possible to calculate the relative intensity of an electron line.

$$I = Ap/y$$

where I ≡ intensity, A ≡ area under the peak produced by the densitometer, and y ≡ efficiency. p is determined by actual measurement, y is read from a curve, leaving only A to be determined.

The following is a modification of the Slätis procedure for finding A. It should be noted that an exact integration to find A is especially complicated by the low-energy "tail" of the electron line.

The electron line shape does not change much with variation of p if the source dimensions are held constant.[7] Instead of using the actual area under the densitometer trace of an electron line a rectangle is taken, the height of which is equal to the density of the peak and the width is the actual width of the line at the point of "half-density." The latter refers to the point where the density,

above fog, is equal to 1/2 of the peak density, also measured above fog. Since only relative determinations are being made any measuring units may be used.

Figure 14 is a reproduction of a densitometer trace of an I^{131} exposure, see also Fig. 15, obtained in PMII. The zero value on the ordinate is obtained by placing an opaque screen in front of the light source and represents zero transmission, e.g., ∞ blackness. The 100 value on the ordinate is obtained by placing an unexposed portion of the film in front of the light source. (Scattered electrons make the density near the line greater than the fog density.)

To obtain the peak height h, R_u is divided by R and the exposure read off the D-E curve (Fig. 13); also R_u is divided by R_o and the exposure read off the D-E curve. The difference of these two exposures equals h. At the midpoint of these two exposures the density $D_{1/2}$ is read from the curve. $D_{1/2} = R_o/R_{1/2}$; from this relation $R_{1/2}$ is obtained. The line width w is measured at a distance $R_{1/2}$ from zero. Then, $A = w \cdot h$.

Slätis found that for two lines that were not strongly exposed the mean error from one measurement of the intensity ratio was approximately 11 percent. If the lines were very strongly exposed R is very small and difficult to measure accurately, and therefore the error is considerably larger.

VI. EXPERIMENTAL

A. I^{131}

I^{131} was used primarily as a calibration standard. However some measurements of interest were made on this isotope. The various conversion electron lines used as standards are listed in Table I. (See Figs. 14 and 15 also.)

In addition four other lines were observed when exposures were made with very active sources. These were the K and L_I lines of a 163.76 ± 0.1-kev transition, the K line of a 177.08 ± 0.1-kev transition, and the L_{II} line of the 80.164-kev transition. The 164-kev level has been assigned to a 12-day isomeric state of Xe^{131}, its energy was determined by Bergström[24] to be 163.9 kev. The 177-kev K line has been sporadically reported[25, 26] but it is not included in the presently accepted decay scheme.[27] These lines were superimposed on the continuous beta spectrum and were too weak to permit the determination of relative intensities. The relative intensities of the K and L_I lines of the 80-kev transition were measured to give a check on the intensity determination method being used. Nijgh, et al.[28] have recently determined this K/L_I ratio to be 6.8. A value of 6.1 was found in this work. The 80.164-L_{II} line had not been previously observed. Mihelich[29] had set an upper limit on its intensity as 10 percent of the L_I intensity. An intensity of approximately 10 percent of the L_I line was determined for the L_{II} line from a densitometer trace. The intensity was definitely less than 15 percent of the L_I line.

This is an M1 transition and the theoretical ratio of L_I/L_{II} is approximately 30.[30]

On one of the I^{131} calibration exposures Auger electron lines were observed in very low intensity. Therefore an I^{131} source with a high activity, several roentgens at one inch, was prepared and run in PMI. Nine Auger lines were observed on this film. It was of interest to measure the energies of these Auger lines.

In an Auger process involving emission of L subshell electrons, an atom, initially ionized in the K shell, undergoes a transition to an atom, doubly ionized in the L shell, and an electron in a free positive energy state. The energy E_{KLpLq} of the ejected electron, no matter what the mechanism of the Auger transition, has a definite quantum value which can be approximately determined by considering the process as an internal x-ray photoeffect,[31] i.e., E_{KLpLq} is given by:

$$E_{KLpLq} = E_K - E_{Lp} - E_{Lq}$$

where $(E_K - E_{Lp})$ is the energy an emitted photon would have had, and E_{Lq} is the Lq subshell electron binding energy. (Lp and Lq denote any two subshells of the L shell, p and q may have any value I, II, or III, and may even be identical.)

Actually, the energy of an Auger electron is more accurately given by:

$$E_{KLpLq} = E_K - E_{Lp} - E'_{Lq}$$

where E'_{Lq} is the binding energy of an Lq subshell electron in an atom already once ionized in one of its L subshells. Experimentally

it has been observed, and it is clearly theoretically consistent with the picture of the Bohr atom, that $E'_{Lq} > E_{Lq}$. The numerical evaluation of E'_{Lq} is a tedious calculation and has been carried out for only a number of light atoms.[32, 33]

Burhop[34] has recommended to use for E'_{Lq} the electron binding energy for an un-ionized atom of the Lq subshell of the element of next higher atomic number. It has been observed experimentally that this correction to the binding energy is too large.[35, 36, 37]

Bergström and Hill[25] made a careful study of the Auger electrons emitted in the decay of K-capturing thallium isotopes. They found that the energy of any KLpLq Auger line is probably to be given, within an accuracy of the order of 1 part per 1000, by the following relationship:

$$E_{KLpLq} = (E_K - E_{Lp})_Z - (E_{Lq})_{Z + \Delta Z}$$

where $\Delta Z = 0.6$ when Lp is L_I, L_{II}, or L_{III} and Lq is either L_I or L_{II}; and $\Delta Z = 0.8$ when Lp = L_I, L_{II}, or L_{III} and Lq is L_{III}. $(E_L)_{Z + \Delta Z}$ is obtained by linear interpolation in the binding energy tables.

There are nine different ways of permuting L_I, L_{II}, and L_{III} in E_{KLpLq}. However, in calculating the energies of the Auger electrons it is apparent that three pairs of transitions have energies so similar that the electron lines would not be resolved in the instruments used in this work.

In an analogous manner the Auger electron energies can be calculated for the case where an L shell electron drops into the K shell and an M shell electron (M_I, M_{II}, M_{III}) is emitted instead of an x-ray.

The Auger electron lines which were experimentally observed, together with their energies, the energies predicted by the Bergström and Hill and Burhop formuli, and the approximate relative intensities are given in Table III. These energy calculations were made for xenon which is the product of I^{131} decay.

It is apparent that the Bergström and Hill formula gives better agreement with the experimentally determined energies than does the Burhop formula.

The relative intensities of the KLL transitions are approximately the same as were observed in mercury by Bergström and Hill,[25] who have pointed out that the experimental values are at variance with the theoretical predictions.

B. Cm^{242}

The decay of Cm^{242} has been studied in several different manners. Prohaska[38] found coincidences between electrons of 37.5 and 25 kev and alpha particles. Using the photographic emulsion technique, Dunlavey and Seaborg[39] observed L and M electrons corresponding to a gamma ray of about 45 kev in coincidence with alpha particles. O'Kelley[40] and Passell[41] using a double-focusing beta spectrometer observed L, M, and N

Table III

Vacancies		Energy (kev) Experimental	E, Bergström formula	E, Burhop formula	Relative intensity
Initial	Final				
K	L_I, L_I	23.50	23.49	23.39	weak
K	L_I, L_{II}	23.83	23.84	23.74	moderate
K	L_{II}, L_I				
K	L_I, L_{III}	24.16	24.15	24.09	moderate
K	L_{III}, L_I			24.06	
K	L_{II}, L_{III}	24.50	24.50	24.44	strong
K	L_{III}, L_{II}			24.41	
K	L_{III}, L_{III}	24.79	24.81	24.76	moderate
K	L_I, M_I	27.88	27.90	27.88	very, very weak
K	L_I, M_{III}	28.07	28.13	28.11	very weak
K	L_I, M_{II}		28.07	28.04	
K	L_{II}, M_{III}	28.45	28.48	28.46	weak
K	L_{II}, M_{II}		28.42	28.39	
K	L_{III}, M_{III}	28.74	28.80	28.78	weak-moderate
K	L_{III}, M_{II}		28.74	28.71	

conversion electrons which corresponded to a gamma ray of 44.1 kev. Asaro et al.[42] have studied the complex alpha spectrum using a magnetic spectrograph, and they have proposed the decay scheme shown in Fig. 16.

In addition, the beta decay of Np^{238} to Pu^{238} (which is the same product nucleus as is produced in the alpha decay of Cm^{242}) has been recently studied by Slätis, Rasmussen, and Atterling.[43] This group found the energy of the first-excited state of Pu^{238} to be 44.1 ± 0.1 kev.

The reported relative intensities of the conversion electrons corresponding to the 44-kev transition are given in Table IV.

Table IV

L_{II}	L_{III}	M	N	MNO	References
1.37	1.00	--	--	0.74	43
1.92	1.00	0.73	0.16	--	44, 29
1.44	1.00	0.61	0.11	--	41

The ratios of the L subshell conversion coefficients had led to an E2 assignment to the 44-kev transition.

Two Cm^{242} sources were used in this work. One source, of approximately 2×10^7 disintegrations per minute, was plated on a 15-mil silver wire, after I^{131} had been plated on the same wire

for an internal standard. The other source of approximately 2×10^8 disintegrations per minute, was plated on 14-mil platinum wire. All exposures were made on PMI, a long exposure is being made at the present time to search for the conversion electrons emitted in transitions from the second to the first excited state. A reproduction of the plate obtained with the weaker source, with I^{131} present, is shown in Fig. 7 (lower film). A reproduction of a densitometer trace of a Cm^{242} exposure is shown in Fig. 17.

The results for the energy of this transition, in kev, from four exposures in PMI are given in Table V.

Table V

Film No.	L_{II}	L_{III}	M_{II}	M_{III}	N_{II}	N_{III}	O_{III}	M_I
69	44.05	44.08	44.11	44.11	44.11	44.13	-	--
70	44.06	44.09	44.16	44.18	44.13	44.14	44.13	44.16
73	44.05	44.08	44.12	44.11	44.08	44.09	44.08	--
74	44.06	44.07	44.09	44.12	44.08	44.09	44.11	--
Average	44.06	44.08	44.12	44.13	44.10	44.11	44.11	

The best energy value from these measurements is 44.11± 0.04 kev.

The results of the intensity measurements from three runs are given in Table VI.

Table VI

Film No.	L_{II}	L_{III}	L_{II}/L_{III}	M_{II}	M_{III}	M_{II}/M_{III}	N_{II}/N_{III}
70	1.16	1.00	1.16	0.49	0.41	1.20	~~1
74	1.3	1.00	1.3	0.44	0.36	1.22	~~1
77	1.23	1.00	1.23	0.48	0.42	1.15	~~1
Average	1.23	1.00	1.23	0.47	0.40	1.19	~~1

Gellman et al.[30] predict theoretically that the L_{II}/L_{III} conversion coefficient ratio for a 44-kev E2 transition in Z = 92 equals 1.18. The ratio of 1.23 obtained in this work is in excellent agreement with the predicted value which gives a confirmation of the previous E2 assignment.

No theoretical calculations have been carried out for the M and N subshell conversion coefficient ratios but it is of interest to note the similarity of the E2 transition conversion ratios in these subshells compared to the L subshell conversion ratios. The N_{II}/N_{III} ratios were obtained by visual estimation since the lines were weak and not completely resolved.

For the ratio L/MNO Slätis et al.[43] found 3.2/1.0, for L/M/N, Freedman et al.[44] and Passell[41] found 4.0/1.0/0.2, and for L/M O'Kelley[40] obtained an approximate value of 5.

The ratios L/M/N obtained from three exposures in this work were: 2.9/1.0/0.3, 2.4/1.0/0.3, and 2.5/1.0/0.3. The M/N ratios agree as well as might be expected with values that had been obtained previously, since the M and N lines are weak. However, the L/M ratios definitely appear lower than those that have been observed by other workers. One possible explanation is that the electron blackening efficiency of the film is changing quite rapidly in this region, a factor of two between 25 and 40 kev, and there may be some uncertainty in the efficiencies which were used to calculate the relative intensities.

C. Cm^{244}

The decay of Cm^{244} has been studied by Asaro and Hummel.[45] They found two main alpha groups with an energy difference, corrected for recoil, of 43.0 kev. The conversion coefficient of the 43-kev gamma ray was found to be about 500; therefore an E2 assignment was made for this transition. The ground state of the daughter nucleus, even-even, is assumed to be (0+) and on this basis the spin and parity of the first excited state would be (2+). No other work had been done previously on this isotope.

Some preliminary data were obtained for Cm^{244} from one exposure of a source of Cm^{242} and Cm^{244}. The curium was vaporized onto an aluminum plate which was approximately 4 mm wide. The source contained approximately 10^8 and approximately 10^7 disintegrations per minute of Cm^{244} and Cm^{242}, respectively. The upper film shown in Fig. 7 was obtained from this exposure.

This was a wide source and consequently the electron lines had very large low-energy "tails." However, the high energy sides of the L_{II} and L_{III} lines were moderately sharp and energy measurements could be made.

The absolute values obtained for the energies of the L_{II} and L_{III} lines probably were not accurate due to the source width. However, the energy differences of the lines of Cm^{242} and Cm^{244} could be expected to be quite reliable. This difference was 1.22 kev for both the L_{II} and L_{III} lines. The Cm^{242} transition energy had previously been determined to be 44.11 ± 0.04 kev. Therefore, the energy of the first-excited state of Cm^{244} is determined to be 43.89 ± 0.07 kev.

The low-energy tailing of the lines made intensity determinations from this exposure very difficult. However, an approximate L_{II}/L_{III} ratio of 1.3 was obtained for Cm^{244}. This again confirms the E2 assignment to the first-excited state to the ground-state transition since the predicted ratio is 1.18.

D. Am^{241}

The decay of Am^{241} has been the object of many studies. Jaffe, et al.[46] have recently reported on many decay properties. Day[17] has measured the energies of several of the electromagnetic radiations with a curved-crystal spectrometer. Milsted, et al.[47,48] have studied the radiative transitions and conversion electrons emitted in Am^{241} decay. The decay scheme proposed by Jaffe, et al.[46] is shown in Fig. 18.

It was apparent from the data that it would be of interest to determine the relative intensities of the conversion electrons as carefully as possible in a high resolution spectrograph. These data would be of assistance in assigning the multipolarity of the transitions. In addition the accurate energy determinations of Day would permit the use of Am^{241} as a calibration standard for the spectrographs.

A source of Am^{241} containing approximately 10^8 disintegrations per minute was prepared by plating the activity on a 10-mil platinum wire. A reproduction of a portion of a densitometer trace of one of the exposures is shown in Fig. 19.

A total of 41 conversion electron lines were observed on the plate. All except 3 very weak lines were assigned to definite transitions. The energies of the observed lines agreed very well with those reported by Milsted, et al., and no direct energy comparisons will be made. Many of the lines were too weak to permit intensity determinations with the densitometer, therefore the intensities will be discussed in connection with the individual transitions. The energies of the electron lines, the conversion subshells, the subshell binding energies, and the transition energies are given in Table VII. Those lines used as calibration standards are indicated "standard" and no energies for these transitions were determined in this work.

The ratios $L_I/L_{II}/L_{III}$ for the 59.6-kev transition were determined to be 1.2/3.7/1.0 with an uncertainty of about ±15 percent

Table VII

Electron energy (kev)	Subshell	Subshell binding energy (kev)	Subshell transition energy (kev)
20.61	M_I	5.75	26.35
20.97	M_{II}	5.36	26.33
	Average		26.34
Standard 11.61	L_{II}	21.59	33.20
" 15.59	L_{III}	17.61	33.20
" 27.46	M_I	5.74	33.20
" 27.84	M_{II}	5.36	33.20
" 28.77	M_{III}	4.43	33.20
31.69	N_I	1.50	33.19
31.92	N_{II}	1.32	33.24
32.15	N_{III}	1.08	33.23
32.45	N_{IV}, N_V	0.77	33.22
32.87	O_I, O_{II}	0.27	33.14
20.97	L_I	22.41	43.38
21.81	L_{II}	21.59	43.40
25.82	L_{III}	17.61	43.43
37.71	M_I	5.74	43.45
39.05	M_{III}	4.43	43.48
42.36	N_I, N_{II}, N_{III}	1.08	43.44
43.21	O_I, O_{II}, O_{III}	0.21	43.42
	Average		43.44

Electron energy (kev)	Subshell	Subshell binding energy (kev)	Subshell transition energy (kev)
33.10	L_I	22.41	55.51
33.97	L_{II}	21.59	55.56
49.8	M_I	5.7	55.5
50.2	M_{II}	5.4	55.6
51.2	M_{III}	4.4	55.6
	Average		55.54
Standard 37.16	L_I	22.41	59.57
" 37.98	L_{II}	21.59	59.57
" 41.96	L_{III}	17.61	59.57
" 53.83	M_I	5.74	59.57
" 54.21	M_{II}	5.36	59.57
55.13	M_{III}	4.43	59.56
55.74	M_{IV}	3.85	59.59
55.87	M_V	3.66	59.53
58.07	N_I	1.50	59.57
58.25	N_{II}	1.32	59.57
58.49	N_{III}	1.08	59.57
58.79	N_{IV}, N_V	0.77	59.56
59.31	O_I, O_{II}	0.27	59.58
59.53	P(?)	~0.03(?)	--

Electron energy (kev)	Subshell	Subshell binding energy (kev)	Subshell transition energy (kev)
77.37	L_{II}	21.59	98.96
81.40	L_{III}	17.61	99.01
	Average		98.98
13.0	unassigned		
13.97	unassigned		
32.64	unassigned		

in each value. Jaffe, et al. found the ratio $L_I + L_{II}/L_{III}$ to be 4.4 ± 1. Wolfson[49] obtained a value of 6.4 ± 1.3 for the $L_I + L_{II}/L_{III}$ ratio but some contribution of the conversion electrons of the 43.4-kev transition is included. Milsted, et al. determined the $L_I/_{III}$ ratio to be 1/1.2. The latter group did not determine the relative intensity of the L_{II} subshell conversion because they believed that the 43.4-M conversion electrons would be superimposed on the 59.6-L_{II} line and the latter intensity would be artificially high.

In this work the 43.4-M_I line was resolved from the 59.6-L_{II} line and the intensity of the former seemed to be completely negligible compared with the latter. Therefore, no appreciable contribution would be made to the 59.6-L_{II} intensity.

On the basis of the $L_I + L_{II}/L_{III}$ ratio it has been suggested that the 59.6-kev transition is an (E1 + M2) mixture.[41, 46] However, with

the present resolution of the L_I and L_{II} lines it is evident that it is not possible to mix E1 and M2 transitions in a proportion that would produce the observed relative intensities. Since higher multipolarities can be ruled out by life-time arguments, it becomes apparent that the relative conversion intensities experimentally observed for this transition cannot be correlated with the present theoretical predictions.

The relative intensities of the M_I, M_{II} and M_{III} subshell conversion electrons were also measured for the 59.6-kev transitibn. The ratios $M_I/M_{II}/M_{III}$ were determined to be 1.3/3.5/1.0 with an uncertainty of approximately ±20 percent for each value. There are no theoretical predictions available for relative subshell conversions in the M shell but, as was pointed out in the discussion of the decay of Cm^{242}, the similarity of the conversion in the corresponding subshells of the L and M shells is very striking.

The N and O subshell lines of the 59.6-kev transition were not well resolved so only the relative intensities of the total shells were determined.

The total shell conversion ratios $L_\Sigma/M_\Sigma/N_\Sigma/O_\Sigma$ were found to be 1.0/0.3/0.1/~0.03, with an uncertainty of approximately 20 percent for each value.

The relative L subshell conversion intensities were determined for the 43.44-kev transition. The ratios $L_I/L_{II}/L_{III}$ were measured as 1.0/1.0/1.0 with an uncertainty of approximately

±25 percent for each number. Milsted et al. reported values of 0.90/0.96/1.00 for these ratios which is in good agreement with the results of the present work.

It has been suggested that the 43.44-kev transition is an (M1 + E2) mixture.[46, 48] On the basis of the conversion coefficients of Gellman, et al.[30] a mixture of approximately 85 percent M1 and approximately 15 percent E2 would give the experimental relative intensities.

The ratio of total L shell conversion of the 59.6-kev transition to the total L shell conversion of the 43.4-kev transition was 3.2 ± 0.6.

The only other line of sufficient intensity to permit a densitometer measurement was the 33.20-M_I line. The ratio of the intensity of this line to the total intensity of the 43.4-L lines was 0.2 ± 0.04. The L line(s) of the 33.2-kev transition would have been at approximately 10 kev and the protective film coating probably prevented their detection.

It has been observed in two previous cases in this work that the M subshell conversion intensities of a given transition approximately parallel the L subshell conversions for the same transition. It appeared further that the magnitude of the conversion coefficients changed by approximately the same amount in going from L subshell conversion to the corresponding M subshell conversion for the same transition. If these conditions are the same for all transition multipolarities it would appear that the 33.2-kev

transition has largely M1 character with a maximum of approximately 5 percent E2 mixing since the M_I line was $\geq$ 4 times as intense as the M_{II} and M_{III} lines which were of approximately equal intensity. Milsted et al. have studied the conversion electrons of this transition and have reported that it is an (M1 + E2) mixture.[48]

VII. ACKNOWLEDGMENTS

I wish to express my gratitude for the encouragement and assistance of Dr. J. M. Hollander under whose guidance this work was carried out.

I would like to thank Professor J. O. Rasmussen, Jr., for his cooperation and for many helpful discussions.

The aid of Dr. M. I. Kalkstein, especially for his efforts in the development of the spectrographs, is sincerely appreciated. The help of Dr. I. Bergström in the spectrograph development is also acknowledged. I would like to thank Dr. Gerhart Friedlander who kindly supplied the blue prints of the Brookhaven permanent magnet spectrographs. Discussions with Dr. Sigvard Thulin have been very helpful.

I would like to express my appreciation to Professors G. T. Seaborg, I. Perlman, and D. H. Templeton for their helpful comments.

Drs. S. G. Thompson, B. G. Harvey, G. R. Choppin, F. Asaro, and Mr. A. C. Chetham-Strode, Jr., kindly supplied the activities used in the spectrograph studies.

The cooperation of J. T. Vale, L. Hauser, G. B. Rossi, W. B. Jones, W. W. Olson and the crew members of the 184-inch and 60-inch cyclotrons and linear accelerator is gratefully acknowledged.

I would like to thank Mrs. Roberta Garrett and Miss Lilly Goda for the counting of samples.

The assistance of Mrs. Margie J. Hollander in drawing figures and other help is gratefully acknowledged.

The aid of Mr. Louis B. Edwards in performing the various machining operations is appreciated.

The work was performed under the auspices of the U. S. Atomic Energy Commission.

VIII. REFERENCES, Part II

1. Maria Goeppert Mayer, Phys. Rev. 78, 16 (1950).
2. O. Haxel, J. H. D. Jensen, and H. E. Suess, Z. fur Physik 128, 295 (1950).
3. B. H. Flowers, Phil. Mag. 43, 1330 (1952).
4. Aage Bohr and Ben Mottelson, Dan. Mat. Fys. Medd. 27 (16) (1953).
5. Rutherford, Chadwick, and Ellis, Radiations from Radioactive Substances (The MacMillan Company).341 (1930).
6. E. Persico and C. Geoffrion, Rev. Sci. Instr. 21, 945 (1950).
7. W. A. Wooster, Proc. Royal Soc. A114, 729 (1927).
8. B. G. Harvey, unpublished data.
9. P. R. Gray and A. W. Stoner, unpublished data.
10. A. W. Stoner and P. R. Gray, unpublished data.
11. F. F. Momyer, Ph. D. Thesis, University of California Radiation Laboratory Report UCRL-2060 (February 1953).
12. H. B. Mathur and E. K. Hyde, Phys. Rev. 96, 126 (1954).
13. H. Slätis, Arkiv för Fysik, Band 6, 415 (1953).
14. D. L. Meyer and F. H. Schmidt, Phys. Rev. 94, 927 (1954).
15. Gunnar Lindström, Phys. Rev. 83, 465 (1950).
16. H. C. Hoyt and J. W. M. DuMond, Phys. Rev. 91, 1027 (1953).
17. P. P. Day, Phys. Rev. 97, 689 (1955).
18. R. D. Hill, E. L. Church, and J. W. Mihelich, Rev. Sci. Instr. 23, 523 (1952).
19. H. Slätis, Arkiv. för Fysik, 8, 441 (1954).

20. C.D. Ellis and W.A. Wooster, Proc. Roy. Soc. A114, 266 (1927).

21. C.D. Ellis and W.A. Wooster, Proc. Roy. Soc. A114, 276 (1927).

22. Robert A. Dudley, Nucleonics 12, 24 (1954).

23. L. Cranberg and J. Halpern, Rev. Sci. Instr. 20, 641 (1949).

24. I. Bergström, Arkiv för Fysik 5, 268 (1952).

25. I. Bergström and R.D. Hill, Arikiv för Fysik 8, 21 (1954).

26. J.M. Cork, Nucleonics 7, 24 (1950).

27. R.E. Bell and R.L. Graham, Phys. Rev. 86, 212 (1952).

28. G.J. Nijgh, L. Th. Mornstein, and N. Grobben, Physica 20, 243 (1954).

29. J.W. Mihelich, Phys. Rev. 87, 646 (1952).

30. A. Gellman, B.A. Griffith, and J.P. Stanley, Phys. Rev. 85, 944 (1952).

31. E.H.S. Burhop, The Auger Effect and Other Radiationless Transitions, Cambridge University Press, London, 1952.

32. H.C. Wolfe, Phys. Rev. 43, 221 (1953).

33. E.H. Kennard and E. Romberg, Phys. Rev. 46, 1040 (1934).

34. E.H.S. Burhop, op. cit. pp 60 and 75.

35. C.D. Ellis, Proc. Roy. Soc. A139, 336 (1933).

36. J.W. Mihelich, Phys. Rev. 88, 415 (1952).

37. H.R. Robinson and A.M. Cassie, Proc. Roy. Soc. A113, 282 (1926).

38. C.A. Prohaska, Ph.D. Thesis, University of California Radiation LaboratoryUnclassified Report UCRL-1395 (August 1951).

39. D.C. Dunlavey and G.T. Seaborg, Phys. Rev. 87, 165 (1952).

40. G.D. O'Kelley, Ph.D. Thesis, University of California Radiation Laboratory Unclassified Report UCRL-1243 (May 1951).

41. T.O. Passell, Ph.D. Thesis, University of California Radiation Laboratory Unclassified Report UCRL-2528 (March 1954).

42. F. Asaro, S.G. Thompson, and I. Perlman, Phys. Rev. 92, 694 (1953).

43. Hilding Slätis, John O. Rasmussen, Jr., and Hugo Atterling, Phys. Rev. 93, 646 (1954).

44. M.S. Freedman, A.H. Jaffey, and F. Wagner, Jr., Phys. Rev. 79, 410 (1950).

45. Frank Asaro and J.P. Hummel, unpublished data (1955).

46. H. Jaffe, T.O. Passell, C.I. Browne, and I. Perlman, Phys. Rev. 97, 142 (1955).

47. John Milsted, Salomon Rosenblum, and Manuel Valaderes, Compt. rend. 239, 259 (1954).

48. John Milsted, Salomon Rosenblum, and Manuel Valaderes, Compt. rend. 239, 700 (1954).

49. J.F. Wolfson, private communication to I. Perlman (1954).

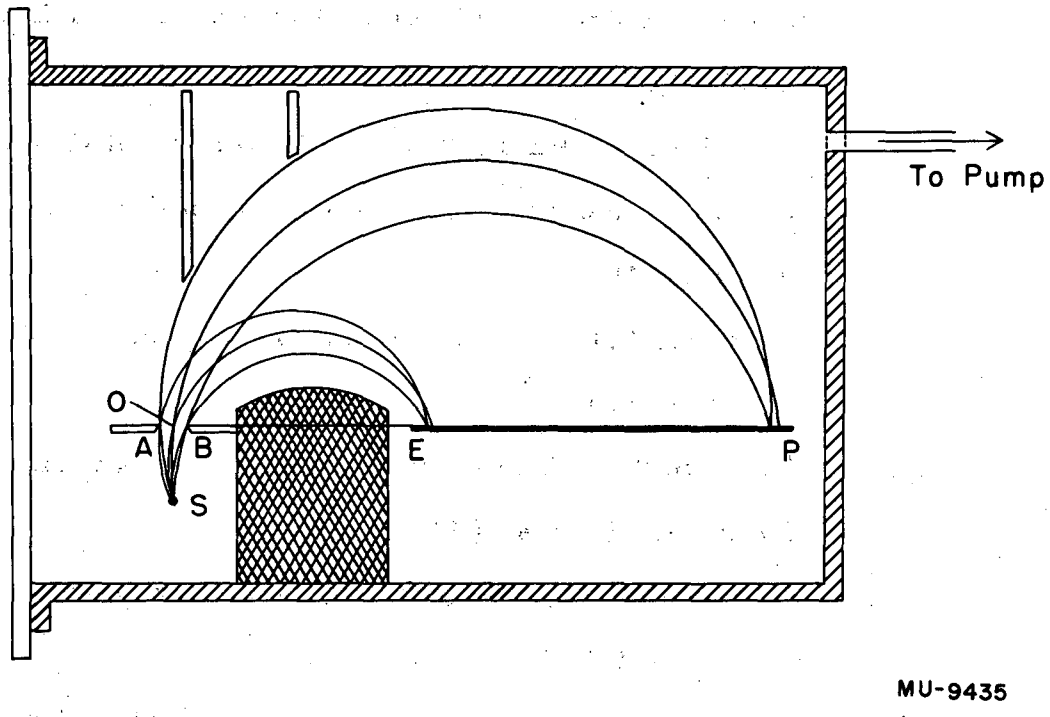

Fig. 1. Schematic drawing of 180° spectrograph.

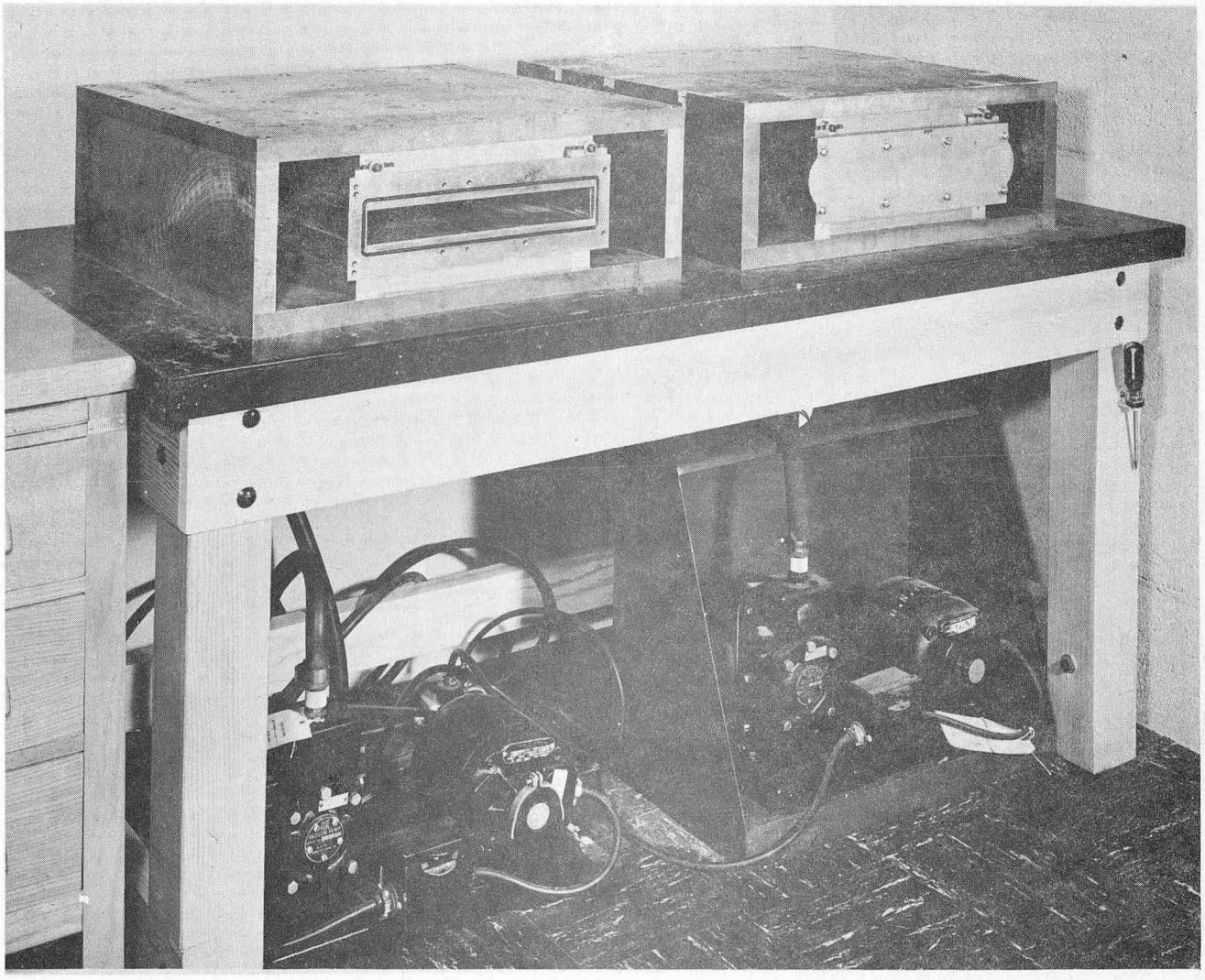

ZN-1249

Fig. 2. Photograph of spectrographs and vacuum pumps. The camera is in position in the magnet on the right, the camera chamber is visible in the other magnet.

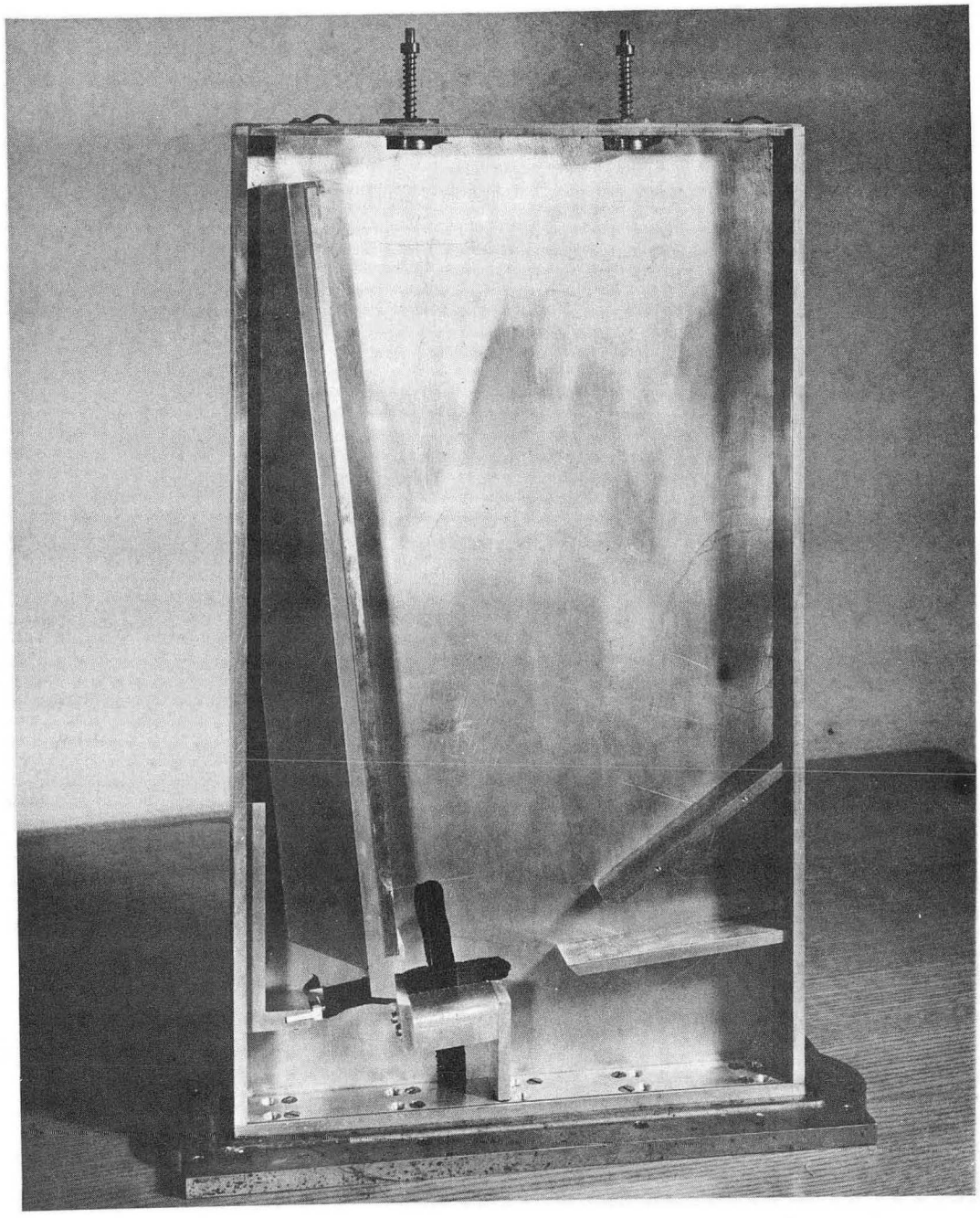

ZN-1250

Fig. 3. Photograph of top view of camera, cover plate removed.

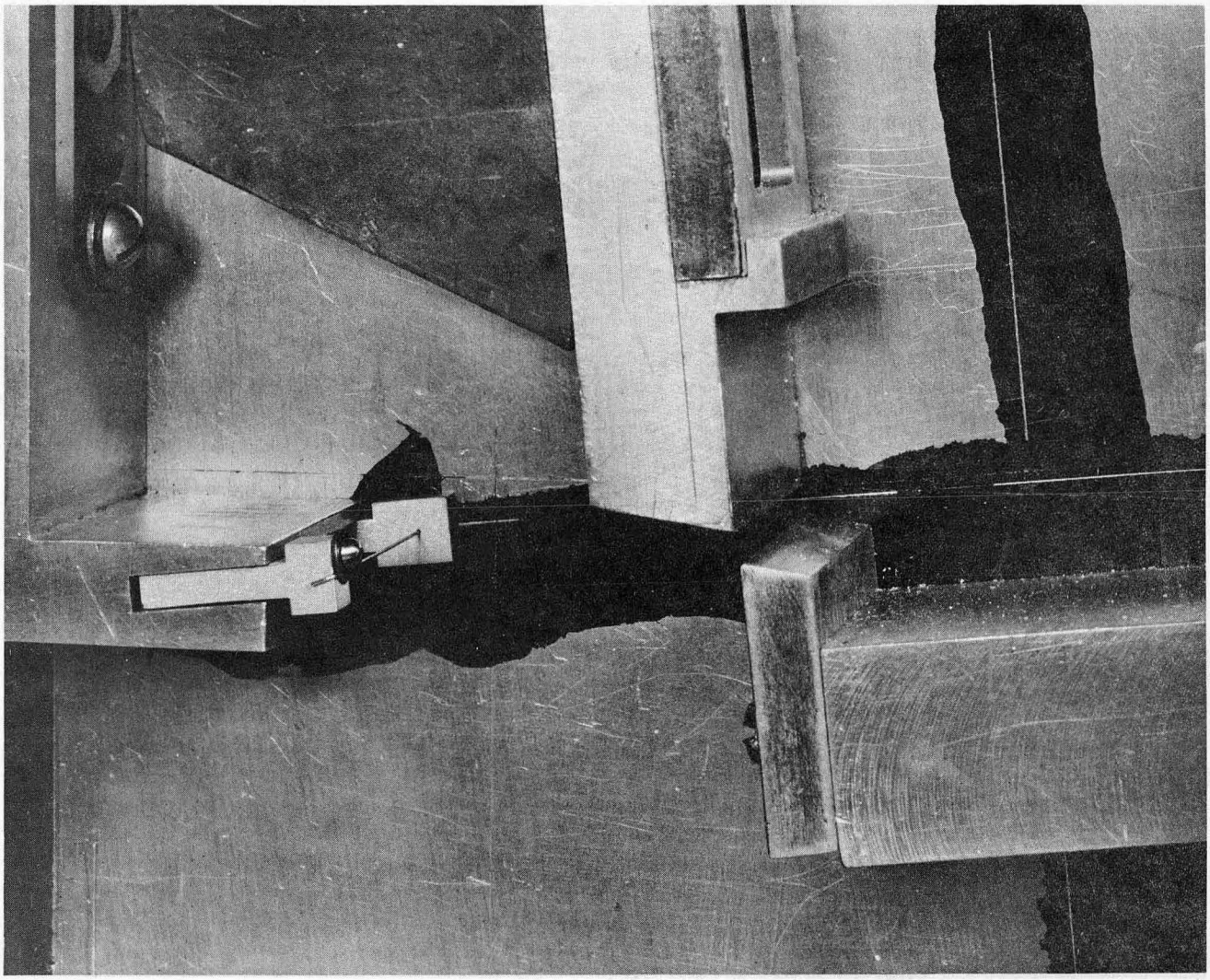

ZN-1251

Fig. 4. Photograph of wire source and collimating slit.

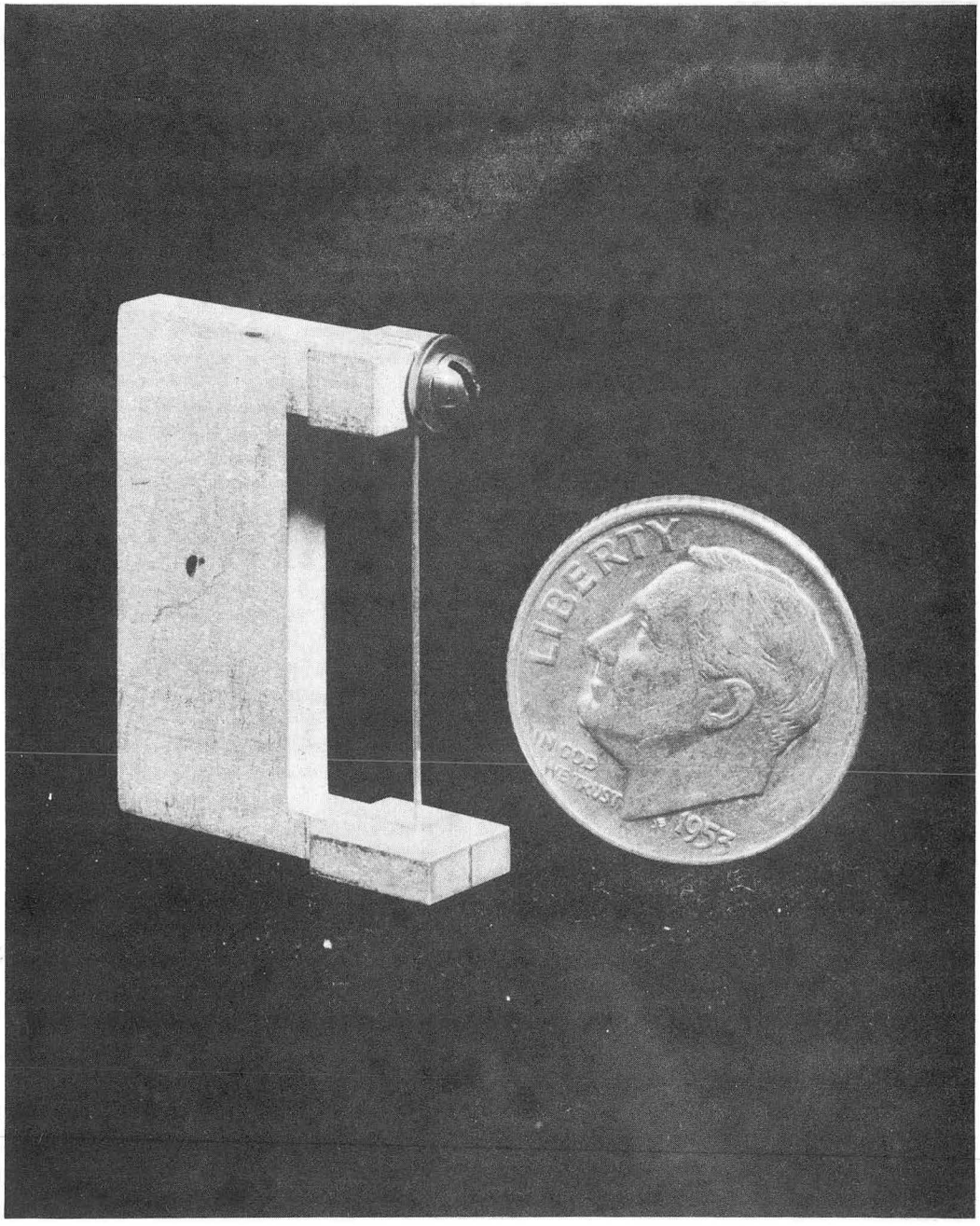

ZN-1252

Fig. 5. Photograph of wire source holder.

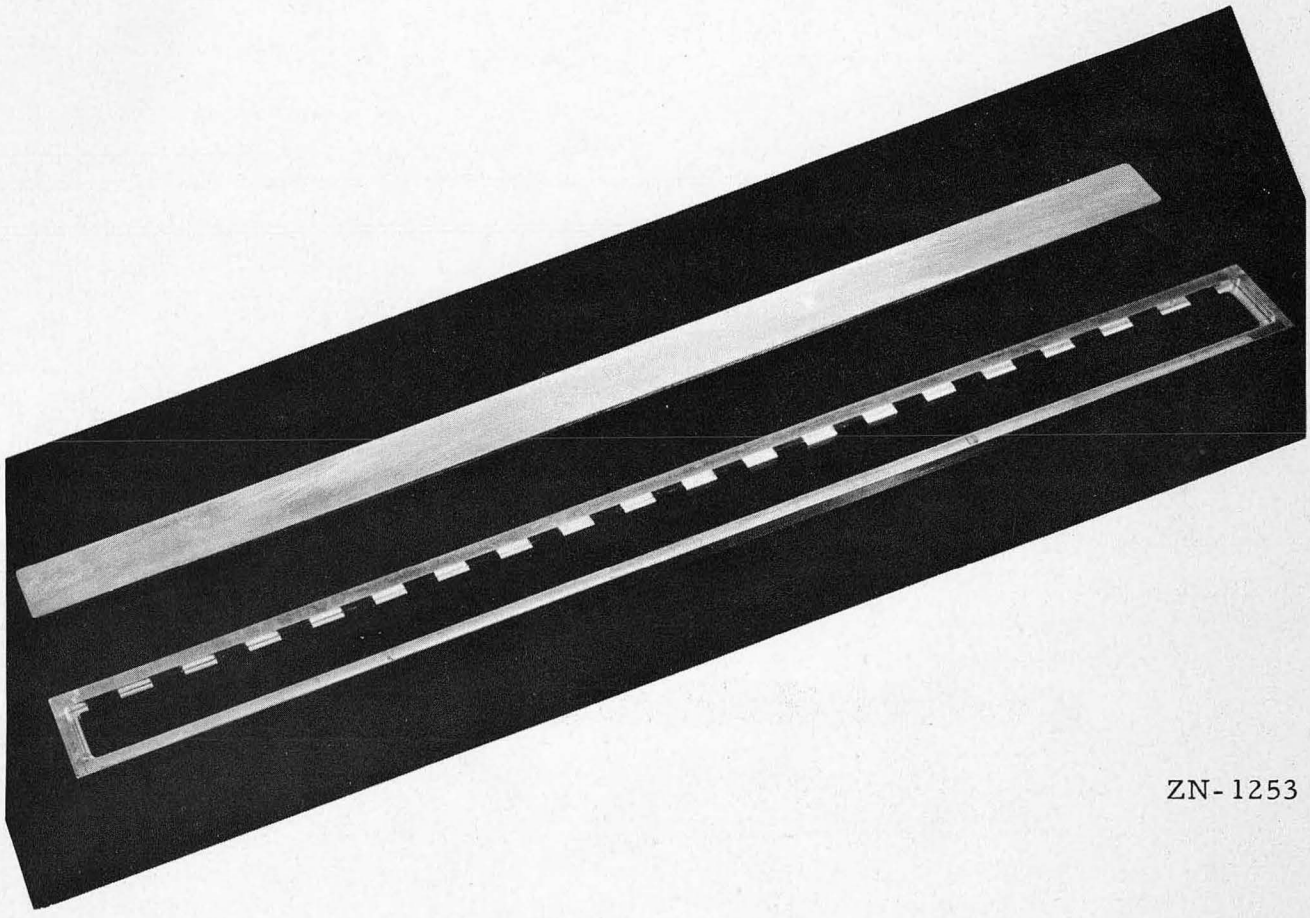

ZN-1253

Fig. 6. Photograph of film holder and rear cover plate for film holder. Calibration notches are visible.

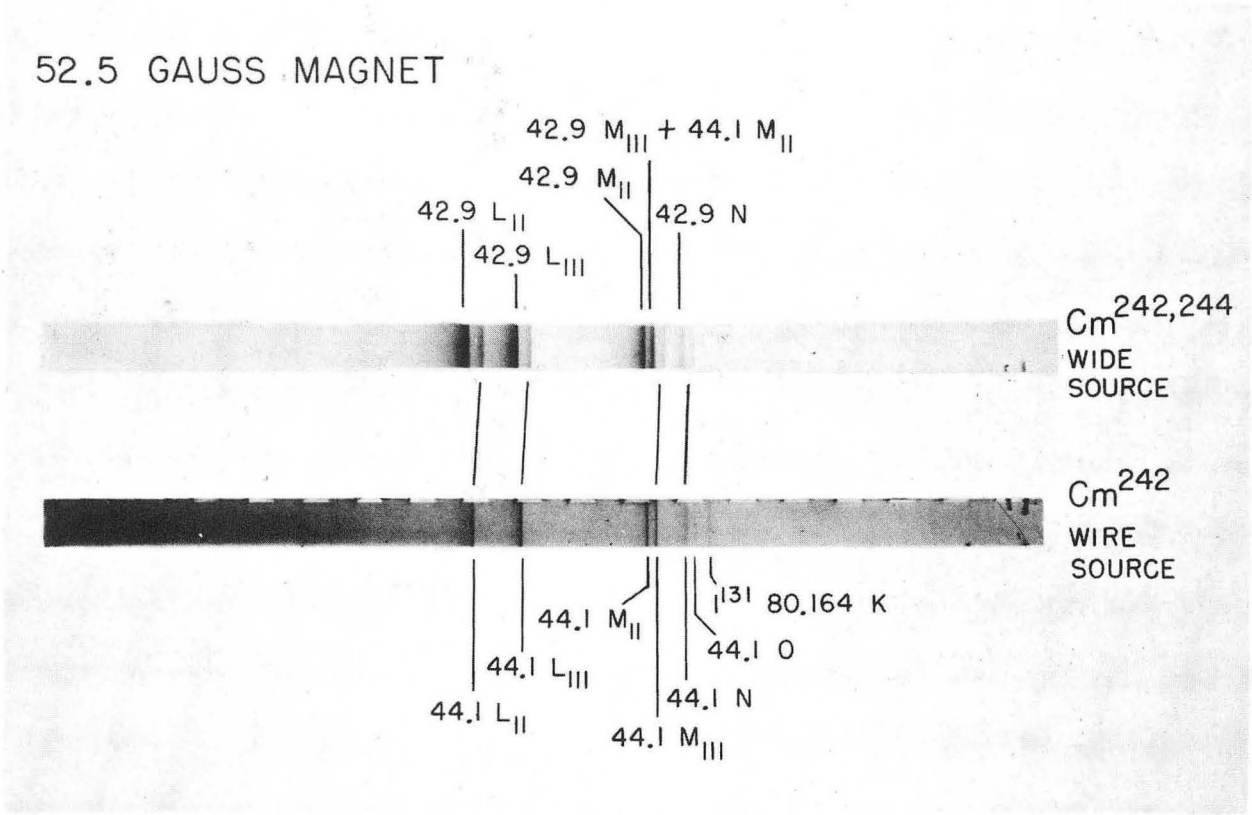

Fig. 7. Photograph of $Cm^{242,244}$ plate (top) wide source, and Cm^{242} plate (bottom) wire source.

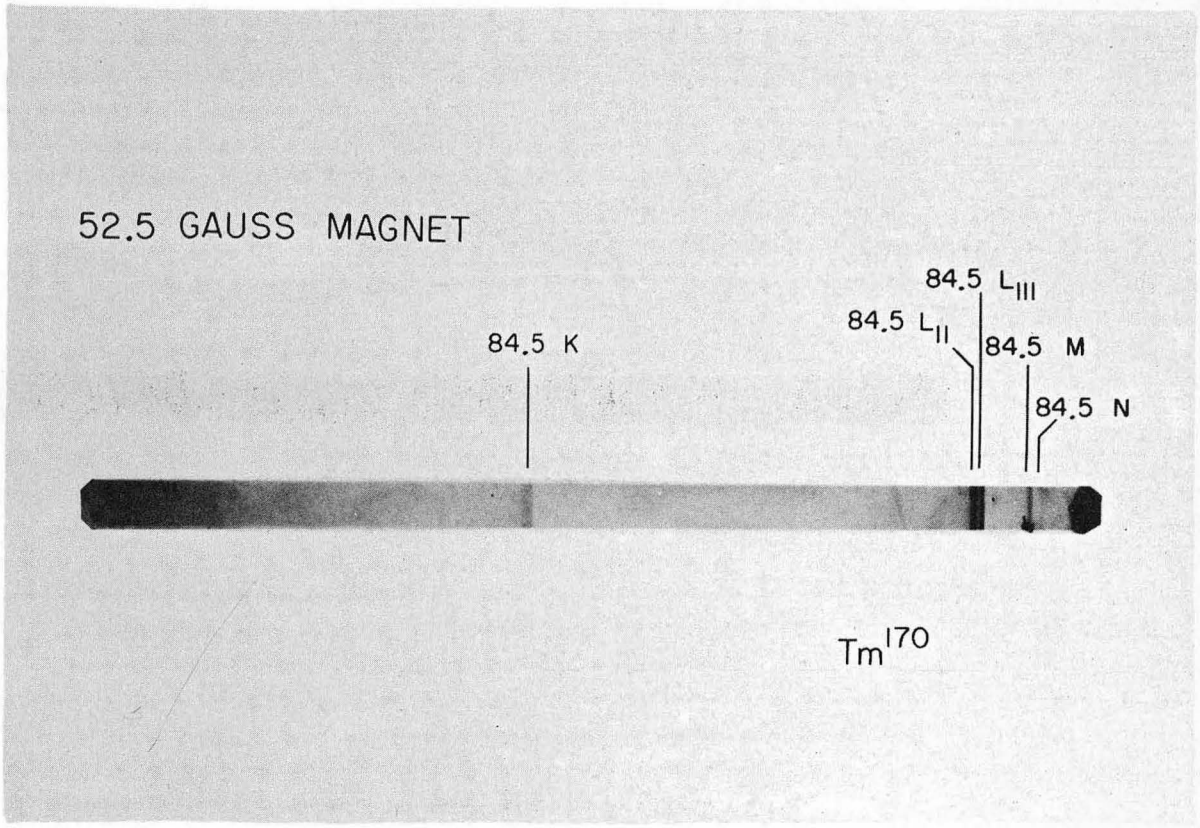

Fig. 8. Photograph of Tm^{170} plate, wide source, cellulose film backing.

ZN-1266

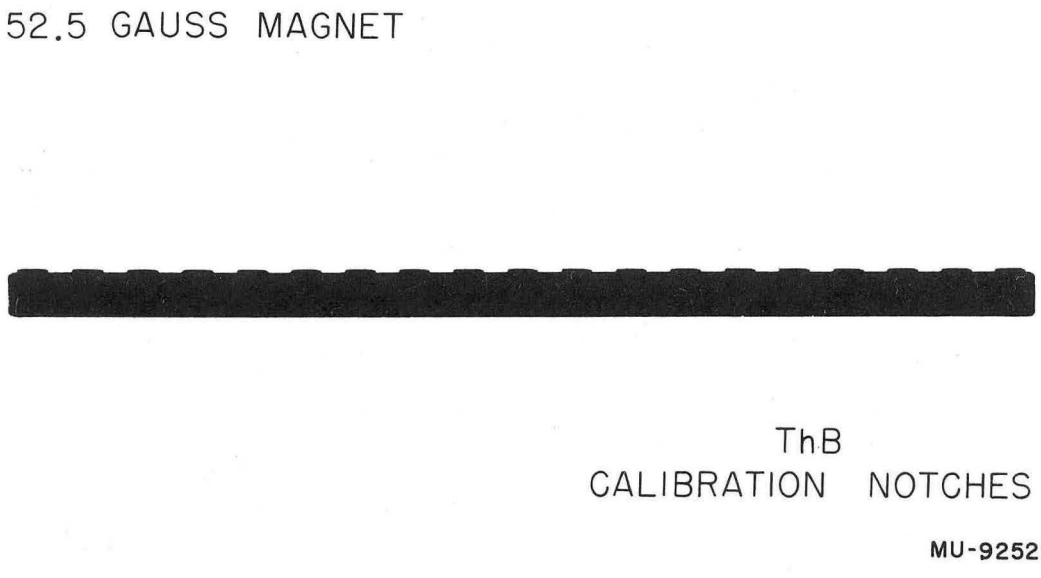

Fig. 9. Photograph of ThB plate. Used to obtain distances between notches on film holder.

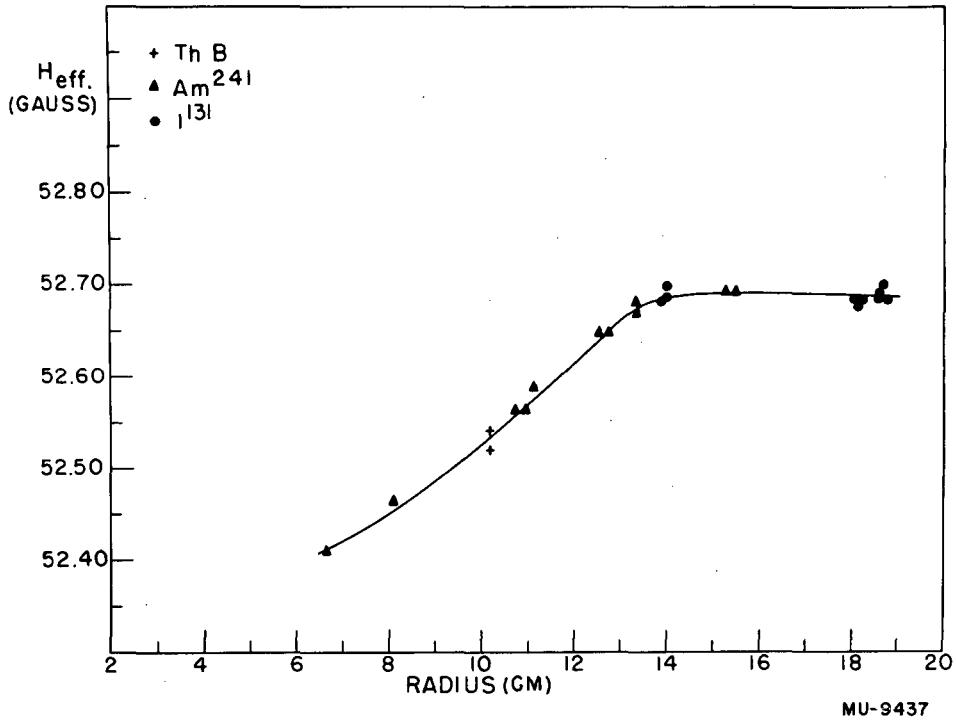

Fig. 10. Calibration curve for PMI. Effective magnetic field, $H_{eff.}$ (gauss) vs electron path radius, p (cm).

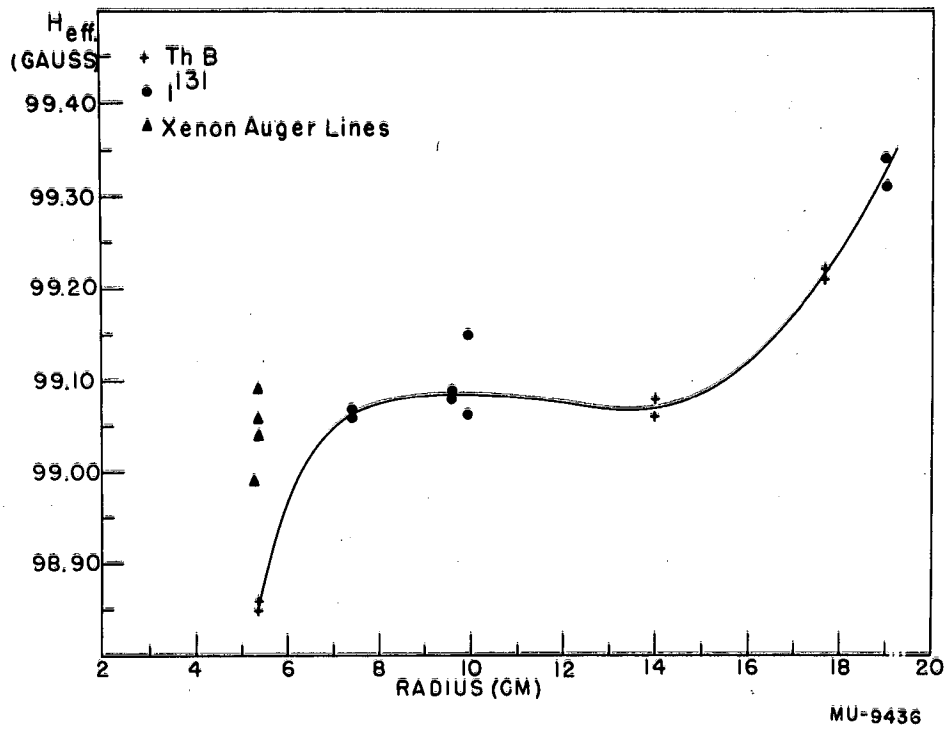

Fig. 11. Calibration curve for PMII. Effective magnetic field, $H_{eff.}$ (gauss) vs electron path radius, p (cm). Xenon Auger lines were not considered in drawing curve.

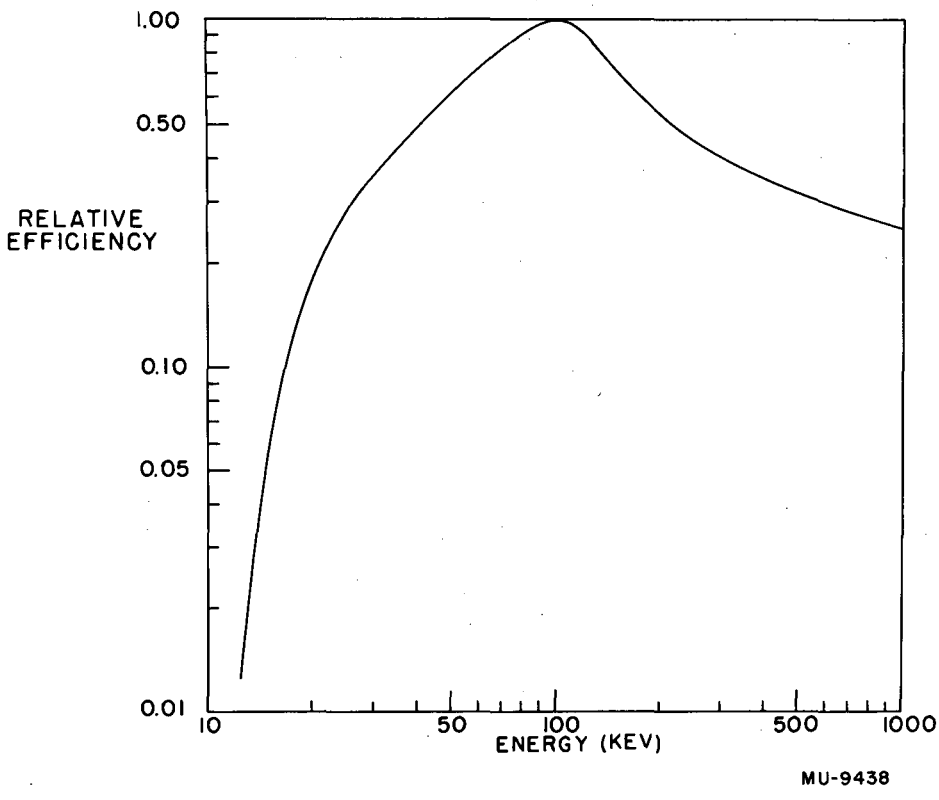

Fig. 12. Electron blackening efficiency, y vs electron energy, e (kev). Dudley[22] and Cranberg and Halpern.[23]

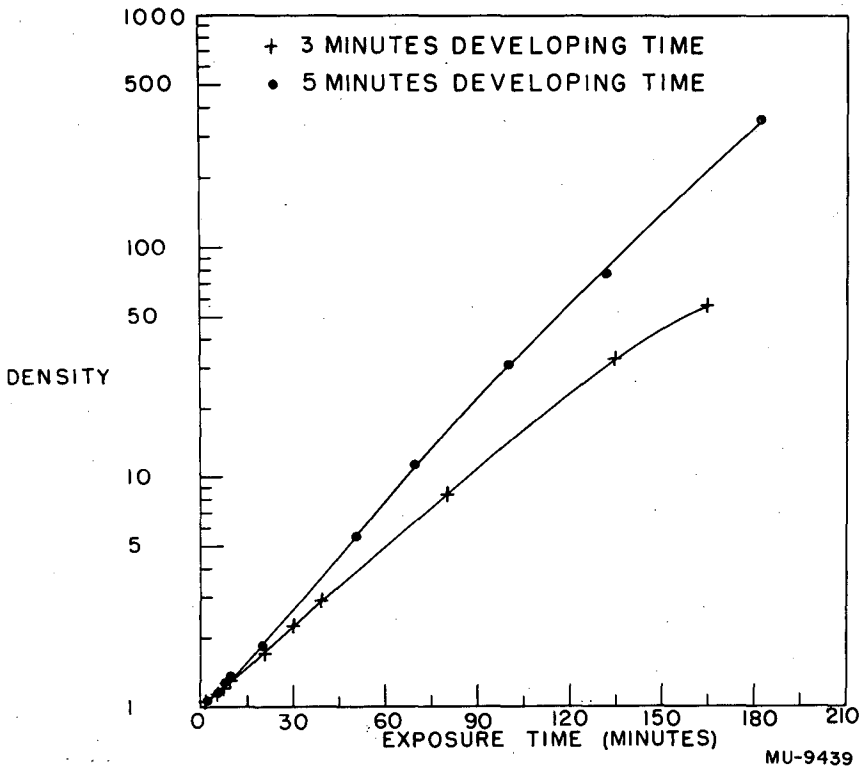

Fig. 13. Density, D, vs exposure, E (minutes). Sr^{90}-Y^{90} source.

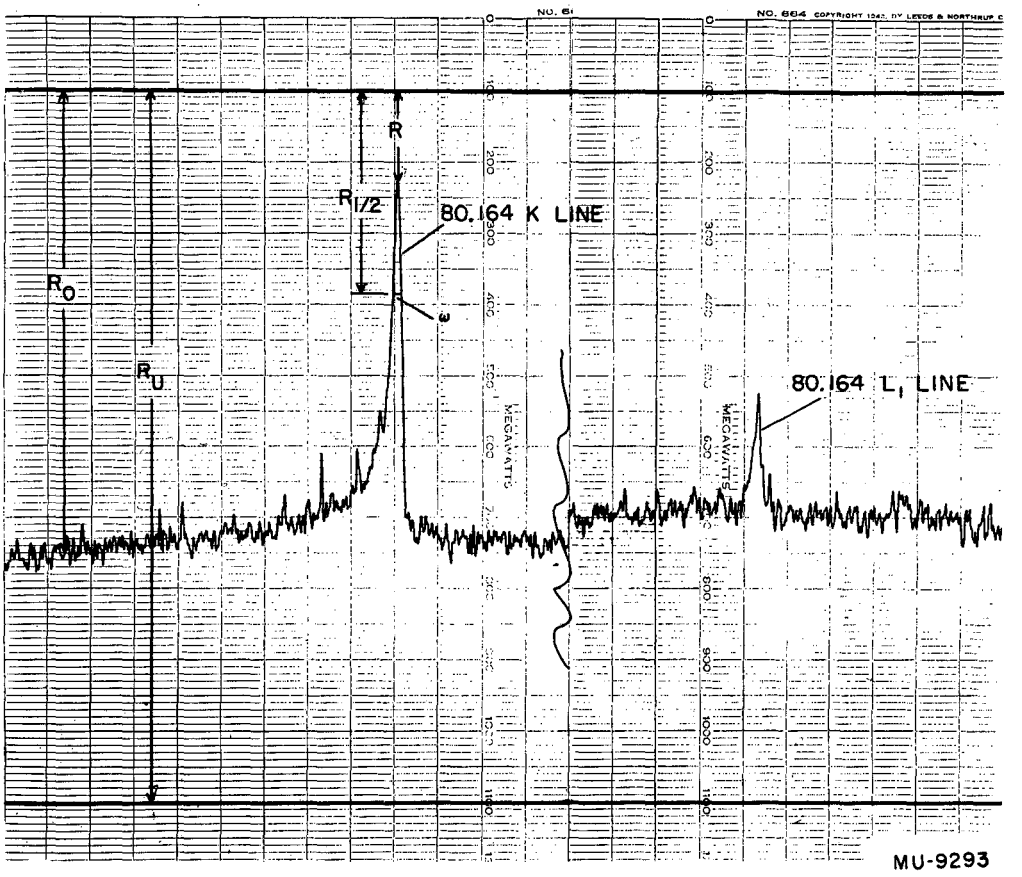

Fig. 14. Photograph of densitometer trace of I^{131} plate. The quantities utilized in the intensity determination, R_o, R, R_u, and $R_{1/2}$ are illustrated.

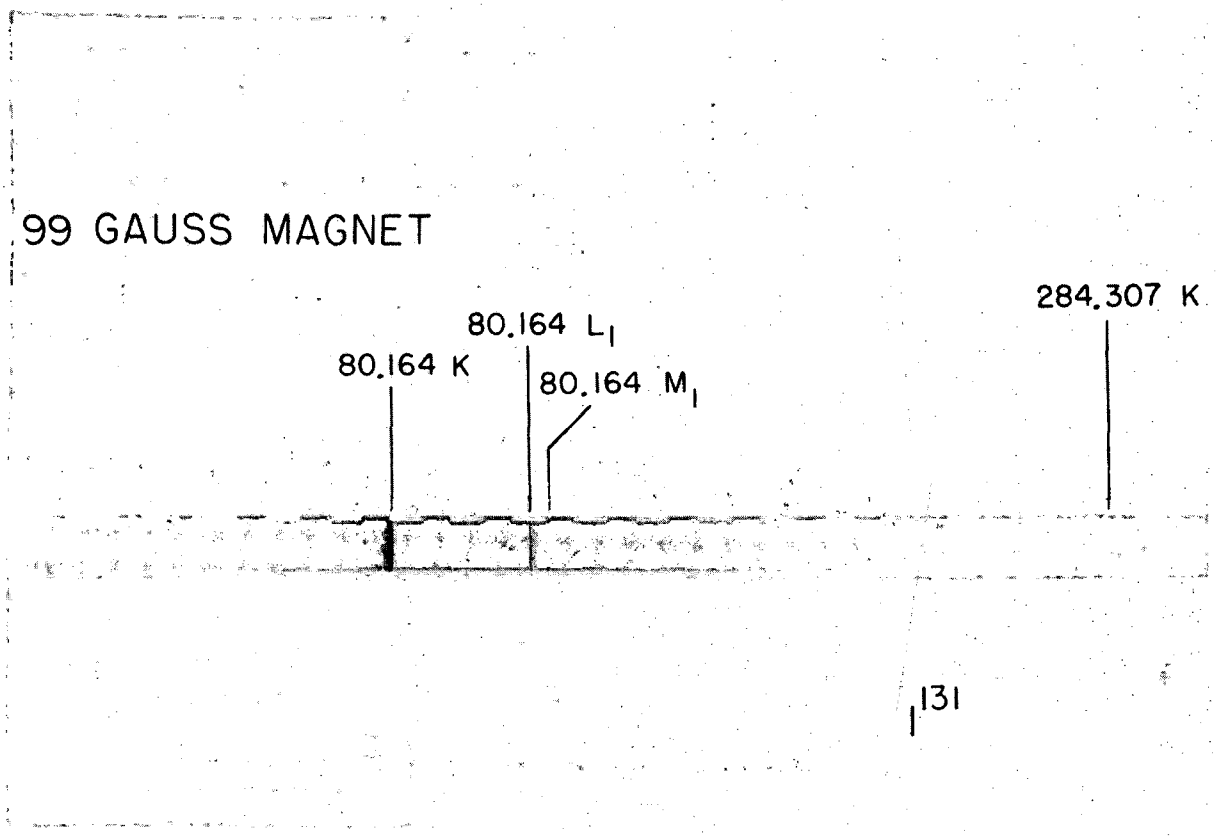

Fig. 15. Photograph of I^{131} plate.

ZN-1268

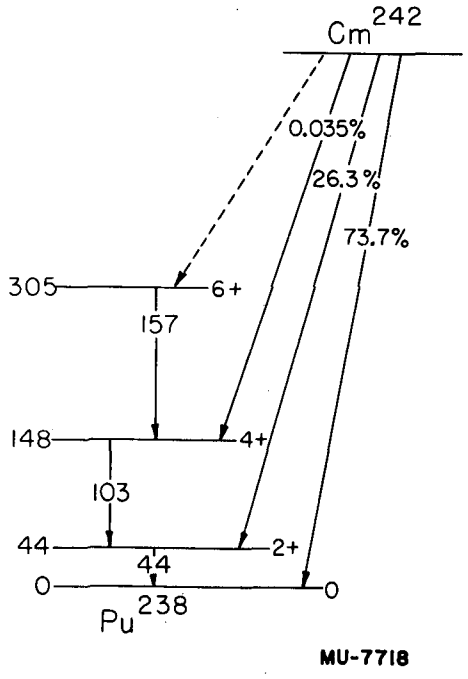

Fig. 16. Cm^{242} decay scheme. Asaro et al.[42]

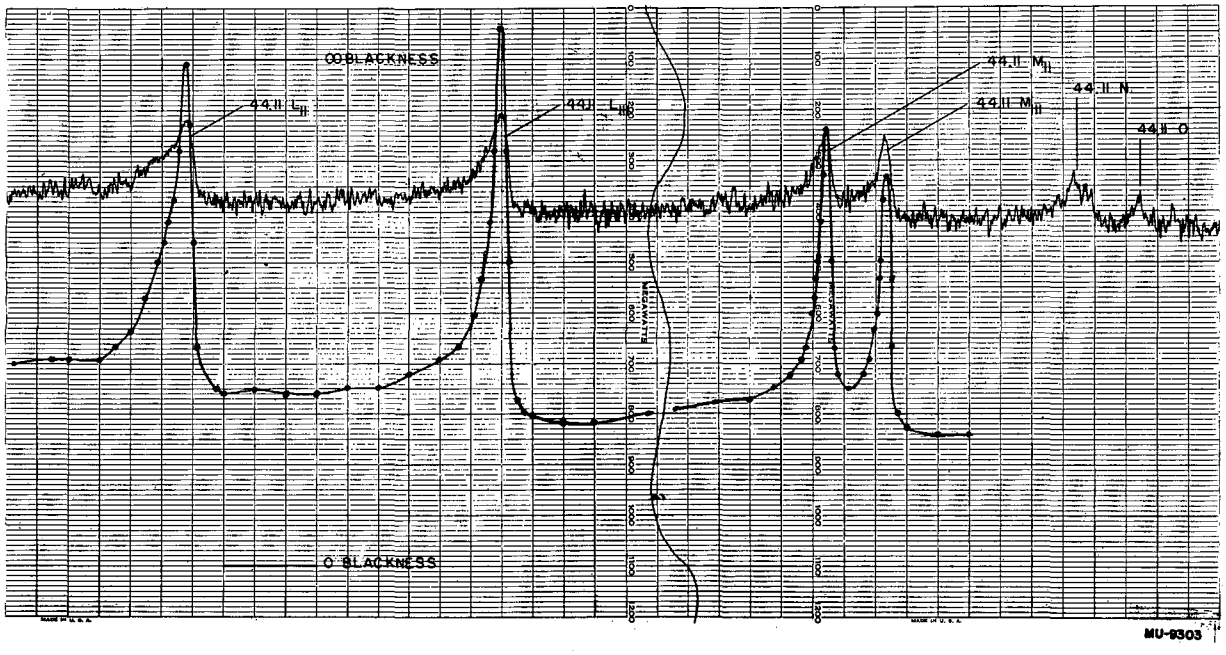

Fig. 17. Photograph of densitometer trace of Cm^{242} plate. The smooth curve passing through the dots represents the relative blackening on a linear scale.

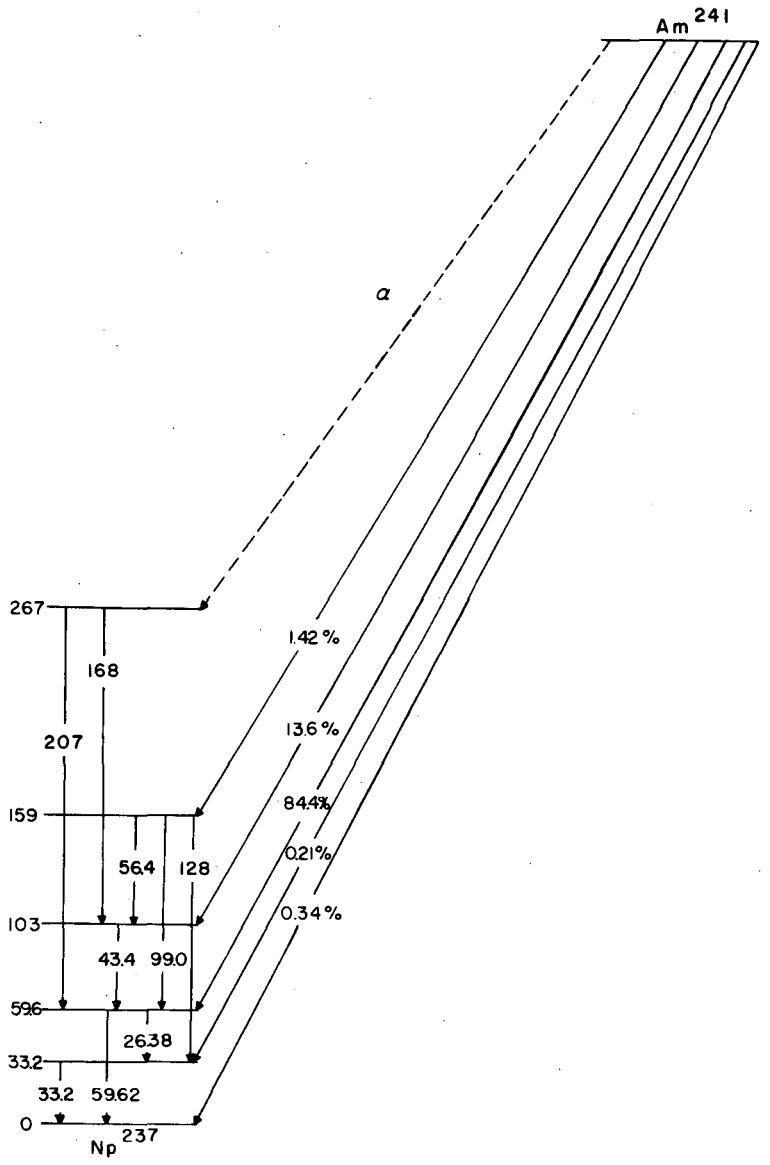

Fig. 18. Am^{241} decay scheme. Jaffe et al.[46]

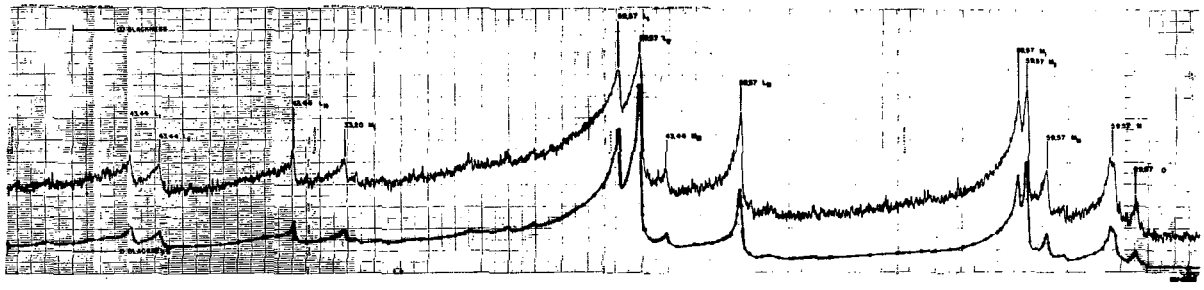

Fig. 19. Photograph of a portion of the densitometer trace of Am^{241}. The smooth curve passing through the dots represents the relative blackening on a linear scale.